

Flexible and smart electronics for single-cell resolved brain-machine interfaces



Cite as: Appl. Phys. Rev. **10**, 011314 (2023); doi: [10.1063/5.0115879](https://doi.org/10.1063/5.0115879)

Submitted: 27 July 2022 · Accepted: 13 February 2023 ·

Published Online: 10 March 2023



Ariel J. Lee,^{1,2} Wenbo Wang,¹ and Jia Liu^{1,a)}

AFFILIATIONS

¹John A. Paulson School of Engineering and Applied Sciences, Harvard University, Boston, 02134 Massachusetts, USA

²Electrical Engineering and Computer Science, Massachusetts Institute of Technology (MIT), Cambridge, 02139 Massachusetts, USA

Note: This paper is part of the special collection on Flexible and Smart Electronics.

^{a)}Author to whom correspondence should be addressed: jia_liu@seas.harvard.edu

ABSTRACT

Brain-machine interfaces (BMIs) offer the potential for the development of communication tools between the brain and external devices. The current BMI technologies for recording and modulation of electric signals from the brain have made significant contributions to areas such as neuroscience, disease diagnosis, and rehabilitation. Next-generation BMIs require long-term stable recording and modulation of electrical signals from statistically significant neuron populations with millisecond single-cell spatiotemporal resolution. However, there are challenges to achieving this stability due to the mechanical and geometrical mismatches between electronics and the brain tissue. In addition, the requirement to achieve cell-type-specific neuromodulation and transmit and process the ever-increasing volume of data *on-the-fly* necessitates the implementation of smart electronics. In this review, we first summarize the requirements, challenges, and current limitations of BMIs. We then highlight three major approaches to the fabrication of flexible electronics as implantable electronics, aimed at enabling long-term stable and gliosis-free BMIs. The progress of multifunctional electronics for multimodal recording and modulation of cell-type-specific components in the brain is also discussed. Furthermore, we discuss the integration of wireless and closed-loop modulation, and on-chip processing as smart electronic components for BMIs. Finally, we examine the remaining challenges in this field and the future perspectives for how flexible and smart electronics can address these problems and continue to advance the field of BMIs.

Published under an exclusive license by AIP Publishing. <https://doi.org/10.1063/5.0115879>

TABLE OF CONTENTS

I. INTRODUCTION	1
II. OVERVIEW OF ELECTRONIC ARCHITECTURES FOR BMIs	3
III. FLEXIBLE ELECTRONICS FOR BMIs	4
A. Thin-layer electronics with flexible substrates	4
B. Intrinsically stretchable and soft electronics	5
C. Tissue-like electronics for seamless integration of electronics with tissues	7
IV. SMART ELECTRONICS FOR BMIs	8
A. Multimodal electronics for recording and stimulating brain activity	8
B. Wireless BMI implants	8
C. BMI implants with on-chip intelligence for closed-loop operation	8
V. OUTLOOK	10
A. Scalability of flexible sensors	12
B. Neuromorphic intelligent BMIs	12
VI. CONCLUSION	13

I. INTRODUCTION

Brain-machine interfaces (BMIs) measure neural signals through devices that directly interface with the brain to interpret brain states^{1,2} [Fig. 1(a)]. While the initial goal of BMI research was to develop assistive devices to restore motor functions in paralyzed parts of the body,^{3,4} recent developments have revealed the broad applications of BMIs across a range of biological and biomedical fields,^{5–7} such as decoding neural activity for basic neuroscience, diagnosing and treating neurological disorders,^{8–10} and advancing the development of neuroprosthetics.¹¹ More recently, BMIs have been applied in non-biomedical fields such as computer gaming and entertainment as well as virtual and augmented reality.^{12–15} All these applications demand the development of BMIs with unprecedented accuracy, efficiency, and longevity.

Most BMIs collect the electrical signals from the brain to decode neural or brain states. There are various types of neural electrical signals that can be recorded, such as electroencephalogram (EEG)^{16,17} and electrocorticography (ECoG)^{18,19} obtained through surface electrodes attached to the surface of the skull or brain tissue. However,

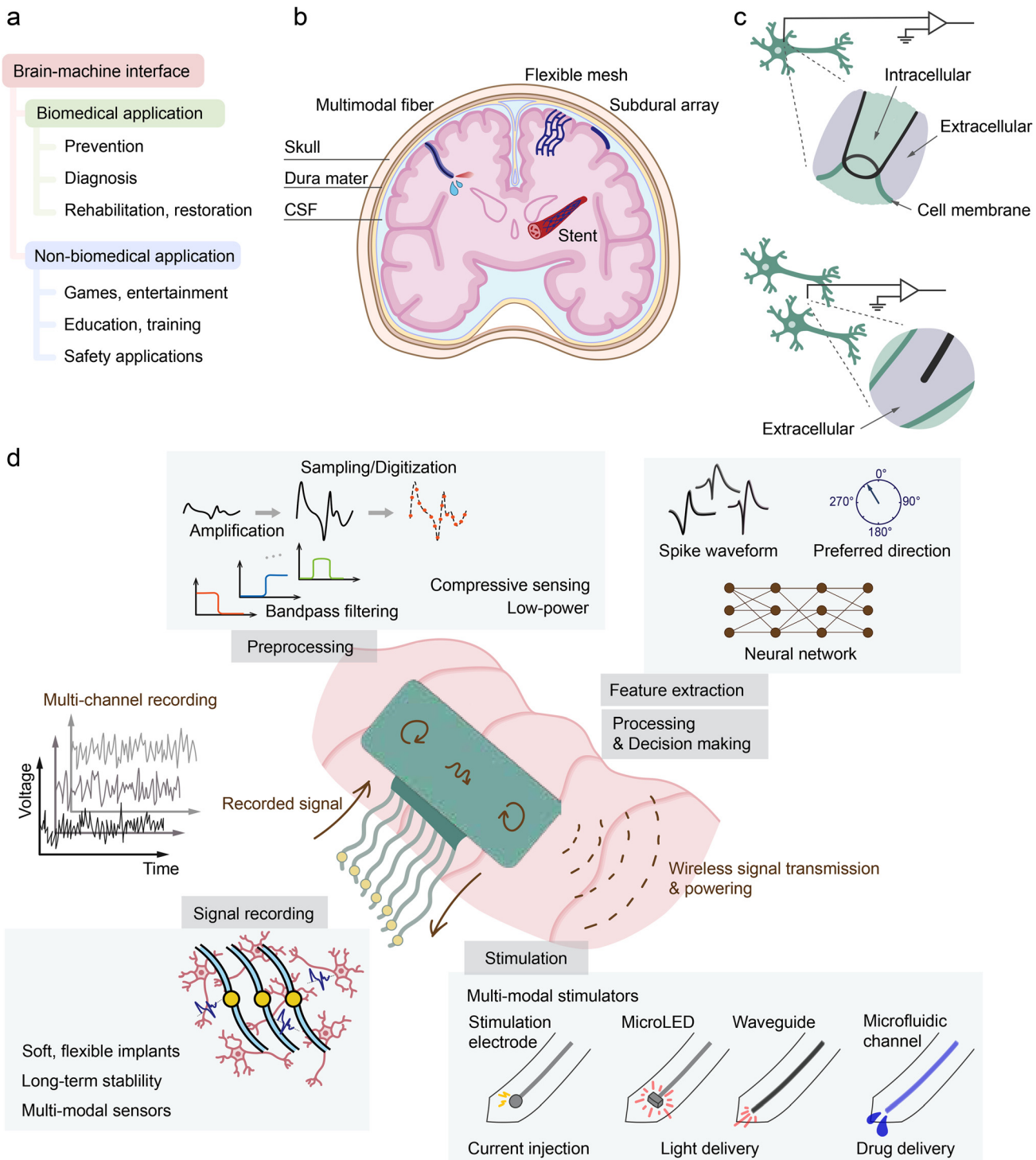


FIG. 1. Overview of the application, type, and components of brain-machine interfaces (BMIs). (a) Various application areas of research on BMIs. (b) Schematics of different flexible electronics for brain electrophysiological signal recording and stimulation. (c) Intracellular electrode disrupts the cell membrane and measures the electrical potential inside the cell (top), and the extracellular electrode measures the electrical potential outside the cell, nearby the cell membrane (bottom). (d) Schematics of the components of a fully implantable wireless, closed-loop BMI. The current research focus and major limitations existing in each component are explained for each component: signal recording, processing, feature extraction, decision-making, and stimulation.

EEG and ECoG, which average signals from millions of neurons, are limited by relatively low temporal and spatial resolution, restricted information for brain state decoding, and signal instability caused by motion artifacts. These challenges make it challenging for surface electrodes to be used for high-resolution and long-term stable BMIs. On the other hand, intracortical electrodes, capable of recording single-unit action potential spikes and local field potentials (LFPs), can potentially address these issues, providing high-throughput and high-bandwidth signal recording with single-cell resolution.²⁰ For example, Michigan probes, Utah arrays, and the recently developed neuropixel probes were designed to record high-density, millisecond-resolved single-unit electrophysiological signals from the brain.²¹

Single-cell neural signals operate at millisecond timescale, while brain-wide activities operate at completely different time scales,^{22,23} taking days, months, or even years to develop. Therefore, effective BMIs must maintain single-cell resolution for recording over an extended period. However, traditional BMIs utilizing intracortical electrodes are highly invasive because the rigid probes containing micro-electrode arrays need to directly interface with individual neurons in the brain tissue to collect data. The significant mechanical and geometrical mismatch between the brain tissue and implanted rigid brain probes introduces chronic mechanical damage to the brain tissue and triggers brain immune responses. Over time, immune cells such as astrocytes and microglia proliferate, leading to degeneration of neurons around the implanted brain probe.^{24,25} Together, these biological changes lead to the degradation of the signals. In addition, the large mechanical mismatch causes the implant locations of the probes to constantly drift inside the brain tissue,²⁶ preventing the conventional intracortical probes from recording the signals from the same neurons. As a result, neural signals need to be constantly calibrated for BMI applications, which prevents the BMIs from operating in a long-term stable manner.

To address the limitations posed by the conventional intracortical probes, recent advancements have introduced the use of flexible electronics for intracortical implantation and neural recording.^{27–30} These flexible electronics are fabricated using thin-film electronics on flexible substrates such as polyimide³⁰ and parylene,³¹ which are designed to reduce the bending stiffness. This thin-film design converts rigid electronic materials into flexible structures with a bending stiffness comparable to individual cells. In addition, using lithographic fabrication techniques, the structure and geometry of the flexible electronics can be designed to mimic the subcellular features of neurons, leading to the creation of “tissue-like” electronics.^{27,32,33} Figure 1(b) shows examples of different designs of flexible electronics for *in vivo* brain electrophysiology. By eliminating the mechanical and geometrical mismatch between the electronics and the brain, the use of flexible and tissue-like electronics allows for gliosis-free implantation, eliminates probe drifting, and enables long-term, stable single-cell recording in behaving animals even throughout the animal’s entire adult life.²⁷

In addition to flexible electronics, smart electronics play a critical role in BMIs. To make BMIs “smart,” two key strategies have been implemented. First, the brain’s states depend on the spatiotemporally orchestrated communications between different types of neurons, defined by their molecular features. As a result, multifunctional electronics are necessary to enable neurostimulation with cell-type specificity.³⁴ To achieve this, various multifunctional electronic and photonic components such as stimulation electrodes, micro-light-emitting

diodes (LEDs),^{35–37} and microfluidic channels^{38–40} have been integrated with flexible implantable electronics to stimulate and manipulate cell-type-specific brain activities based on real-time recording data. Second, as the volume of recording data continues to grow, the need for electronic circuits that are capable of on-site, real-time data analysis, compression, and wireless transmission as well as data processing for stimulation control has been increasing. To meet this need, machine learning (ML) algorithms, artificial intelligence (AI)-driven circuits, and neuromorphic devices have been integrated into BMIs to facilitate on-chip data processing. By combining smart electronics with flexible electronics, BMIs can be enhanced with multifunctional and multimodal recording and control capabilities as well as on-site data processing and analysis. These advances are crucial for the next-generation BMI technology.

In this review, we discuss recent progress in the field of flexible and smart electronics that advances the capability of BMIs, with a focus on invasive BMIs that are capable of decoding brain activities based on single-cell resolved signals. We first highlight latest developments in flexible electronics, covering three key strategies for the fabrication of flexible implantable electronics to enhance recording stability. Then, we review advances in multimodal electronics that enable targeted closed-loop recording and cell-type-specific stimulation of the brain. We also review bioelectronics that incorporate on-chip intelligence for data processing and transmission, including wireless operation. Finally, we discuss the potential of flexible electronics with high-density electrodes and neuromorphic electronics as promising research directions, which will enable the creation of long-term stable, high-density, and high-throughput BMIs with real-time decision-making capabilities.

II. OVERVIEW OF ELECTRONIC ARCHITECTURES FOR BMIs

The electrical activities of nervous systems are generated by the transient changes in the neuronal cell membrane potential resulting from ion movements. The single neuron firing event, known as “action potential,” can be measured using various technologies such as micro-electrodes,^{41,42} field-effect transistors,^{43,44} or membrane-located voltage indicators.⁴⁵ In this review, we focus on the electrode-based electrical recording, as it remains the only technique demonstrated for human BMI applications. These electrode-based neural interfaces can be categorized into two types: intracellular and extracellular interfaces [Fig. 1(c)]. Intracellular electrodes (e.g., patch-clamp and nanopillars) permeabilize the cell membrane to measure the electrical potential inside the cell. Because intracellular electrodes are physically in contact with the cytoplasm, they can record and stimulate neural activity with a high spatiotemporal resolution and high signal-to-noise ratio (SNR), with patch-clamp considered as the gold standard for neural activity characterization. However, the intracellular electrical recording process also damages the neuron membranes and limits long-term stability for electrical measurement. In addition, while intracellular measurement has been scaled up to simultaneously record thousands of cells *in vitro*,⁴⁶ the scalability of current intracellular technologies for *in vivo* measurement is still limited. In contrast, extracellular electrodes do not puncture the cell membrane and record action potential outside the cell. Extracellular electrodes, thus, introduce minimal damage to neurons, which gives the opportunity for long-term recording and stimulation of neural activities. However, the electrical coupling

efficiency of extracellular electrodes is compromised by the membrane resistance and leakage current. Consequently, the amplitude of the extracellular signal is much smaller than that of the intracellular signal, and the stimulation efficiency is low. Therefore, signal amplification systems are important for extracellular recordings to acquire high SNR signals. Also for electrical stimulations, high current is needed. To scale up the number of electrodes simultaneously recorded, a multiplexing circuit is typically required. Moreover, extracellular electrodes can capture signals from multiple neurons near the electrode. To isolate and assign the action potential events (spikes) to each neuron, a spike sorting algorithm needs to be implemented.^{47,48} A typical BMI for extracellular recording and stimulation, therefore, consists of a sensing electrode array for neural signal collection, integrated circuits for signal processing and analysis, and stimulators for feedback or external controls [Fig. 1(d)].

The interface between the electrodes used for sensing and stimulating the brain tissue is crucial as these electrodes must be implanted into the brain tissue and directly interface with neurons.⁴⁹ Despite the great success, a group of failure modes have limited the further application of the traditional electrode-to-neuron interfaces for long-term stable recording. First, corrosion is caused by the electrochemical reactions of metal probes at the interface when exposed to biological fluid containing various ions and anions, which accelerate the electrochemical reactions^{50,51} [Fig. 2(a)]. The corrosion will not only decrease the signal quality but also release metal ions that trigger toxic reactions.^{52,53} Notably, some electronic components such as transistors are extremely sensitive to the penetrated ions.^{54–56} A common strategy to reduce corrosion is to employ insulating materials such as Al₂O₃,⁵⁷ parylene,⁵⁷ SU-8,²⁷ polyimide,⁵⁸ etc. to isolate the metal component from the saline environment, termed as “passivation layer” [Fig. 2(e)]. Second, the significant mechanical and geometrical mismatch between rigid probes and neurons leads to micromotion-induced probe drift in the brain⁵⁹ [Fig. 2(b)]. Probe drift could further chronically damage the brain tissue and make the single-cell level signal recording unstable. In addition to recording, many clinical treatments for brain disorders and dysfunction require long-term stimulation of specific neurons within targeted brain regions.^{9,60,61} The probe drift and micromotions will move the stimulation probe away from the original position, preventing the device from stable stimulation of targeted neuron populations. Third, the mechanical mismatch will breach the blood-brain barrier (BBB) [Fig. 2(c)]. BBB is the blood vessels that vascularize the central nervous system (CNS) as a semipermeable membrane, which allows these vessels to tightly regulate the movement of ions, molecules, and cells between the blood and the brain with very high selectivity.^{62,63} Insertion of the probe can disrupt the BBB, resulting in the influx of blood-serum protein and subsequent immune inflammation, glial activation, and neuronal degeneration.^{63–65} Fourth, the mismatch will trigger corresponding immune responses and cause gliosis during long-term implantation.⁶⁶ For example, it will trigger the mechanical activation of astrocytes and microglia. The proliferation, migration, and accumulation of these immune cells form a scar sheath around the implanted probe that is 50–200 μm thick, which then isolates the recording region from neurons, leading to a significant loss of SNR [Fig. 2(d)]. Moreover, BBB breach and the immune response increase the chance of the chemical corrosion of the brain probe. The combination of these failure modes prevents the rigid brain probes from recording the activity of the same

neuron in a long-term stable manner. As the mechanical and geometrical mismatch is the major limitation, introducing thin-film electronic structures, low modulus electronic materials, or biomimetic structure designs to brain implantable electronics, which would enable tissue-level-flexible and soft bioelectronics, could substantially reduce the mechanical rigidity and feature dimensions of the electronics [Figs. 2(f)–2(h)].

III. FLEXIBLE ELECTRONICS FOR BMIs

Flexible electronics have mechanical properties that are like those of biological tissues. Thus, their contact with cells and tissues results in minimal mechanical disruptions and damage. The development of flexible implantable electronics can reduce the damage incurred during implantation, eliminate probe drift or micromotion,⁵⁷ and reduce the foreign body response.⁶⁷ In this section, we highlight three general methods to design flexible implantable electronics.

A. Thin-layer electronics with flexible substrates

As the bending stiffness of the device is proportional to the cube of its thickness,³² rigid electronics can be made into flexible electronics by substantially reducing their thickness.^{73–75} Recent studies have shown that by using flexible electronics as implanted electronics, the chronic mechanical damage and immune response can be significantly reduced, allowing for long-term recording of neural activities.^{65,67,76,77} For example, Chung and co-workers integrated modular polymer electrode arrays on a polyimide film substrate.⁵⁸ The thin-layer devices were then stacked to support up to 1024 channels with a total thickness of only 14 μm [Fig. 3(a)] with a field programmable gate array (FPGA) headstage for synchronizing modules and data conversion [Fig. 3(b)]. Because of the reduced mechanical mismatch and immune response, this integrated system can record from hundreds of single units across multiple brain regions in freely behaving rats and can maintain stable recording for more than 160 days [Fig. 3(c)]. Moreover, Luan *et al.* developed a nanoelectronics thread with multilayer, substrate-less architecture with subcellular dimensions to reliably detect and track a single unit for months.⁷⁸ In addition to the traditional design for long-term recording, recent advances in materials science and electronic design also give flexible electronics additional capabilities and optimization opportunities. For example, Zhao *et al.*⁷⁹ have developed ionic communication devices that operate by generating and sensing the electrical potential energy in the physiological environment by ions in the frequency domain. This device can record and transmit the neuron data in freely behaving rats for several weeks in a noninvasive manner. Khodagholy *et al.*³¹ used ultrathin and conformal poly(3,4-ethylenedioxythiophene):polystyrene sulfonate (PEDOT:PSS) electrodes with parylene C as an encapsulation substrate [termed “NeuroGrid,” Fig. 3(d)] for recording LFP and action potential at the superficial layer of the rat cortex with more than 1-week durability in freely moving rats [Fig. 3(e)]. Aside from traditional materials, electronics based on novel materials such as graphene-based transistors has also been employed for mapping brain activities. For example, Masvidal-Codina *et al.*⁶⁸ developed a graphene-based flexible transistor array with 10-μm-thick polyimide as flexible substrates [Fig. 3(f)]. This device achieves high-resolution mapping of cortical activity at infraslow frequencies (<0.1 Hz), which is hard to achieve with traditional electronic design due to the voltage drift and high-electrode

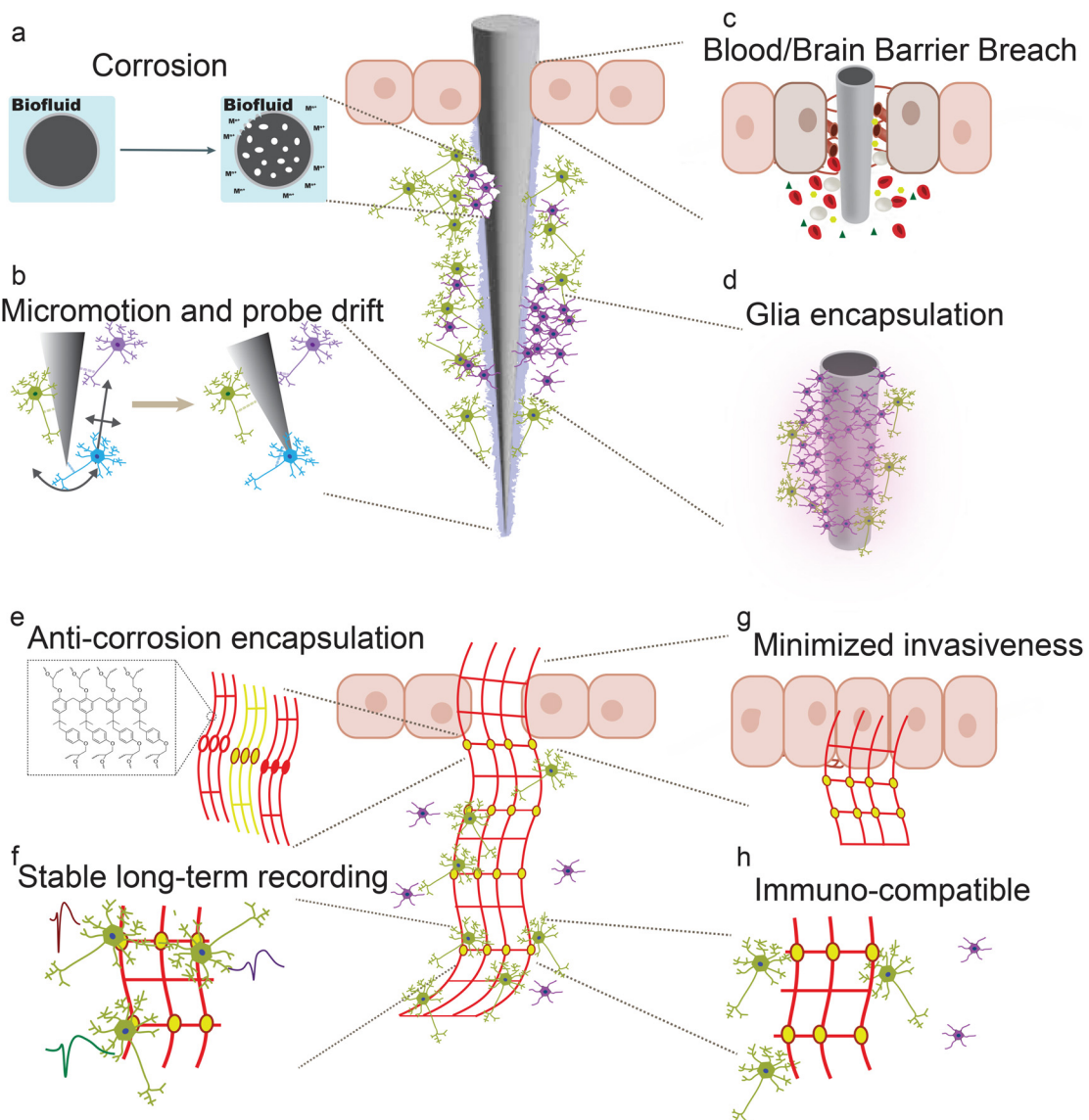


FIG. 2. Failure modes for traditional neural implants. [(a)–(d)] Schematic showing the failure modes of traditional neural implant probes. (a) Coating failure and corrosion due to interface electrochemical reactions. (b) Micromotion and probe drift cause the probe away from the original place. (c) Blood–brain barrier breach induces an influx of blood cells and blood–serum proteins that induce immune inflammation, further causing glial activation and neurodegeneration, and (d) the scar formed by glial encapsulation separates electrodes from recorded neurons, which leads to a decrease in SNR. [(e)–(h)] Flexible electronics pave (mesh electronics are used as an example) the way for resolving failure modes of traditional neural implants. (e) Effective coating of insulating materials (SU-8 as an example) as passivation layers enables anti-corrosion capability. (f) Long-term stable recording by reduced mechanical mismatch. (g) Minimized blood–brain barrier (BBB) breach with flexible electronics. (h) Mitigate gliosis by improved softness and open-architecture design.

impedance [Fig. 3(g)]. All these results show the potential of thin-layer-based flexible electronics as powerful BMIs.

B. Intrinsically stretchable and soft electronics

In addition to reducing the devices' thickness, using intrinsically soft electronic materials to build an implantable brain probe could further reduce the mechanical rigidity of the devices.^{80–84} For example, Minev *et al.*⁶⁹ developed a flexible and transparent polydimethylsiloxane

(PDMS)-based neural probe with soft platinum electrodes and gold interconnects for recording the electrical activities from the cortical surface [Figs. 3(h) and 3(i)]. This allows the reconstruction of the cortical activity map through ECoG [Fig. 3(i)]. The device can be further implanted into the spinal sub-dura region of a rat, functioning as an “electronic dura mater” for neuroprosthetic interface applications. In addition, conductive polymers show both ionic and electronic conductivities, which can be coated to the surface of the electrode to reduce the electrochemical impedance to enhance the SNR of recording.^{82,85–89}

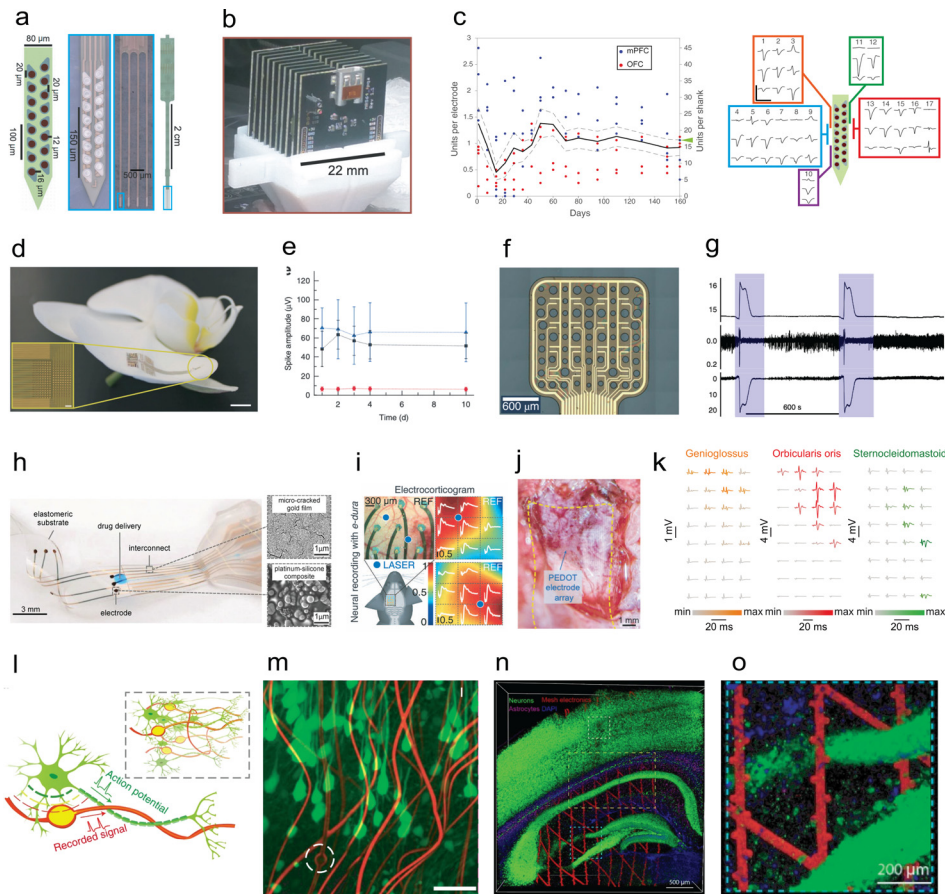


FIG. 3. Structure and material strategies for flexible implantable electronics. [(a)–(g)] Thin-film flexible electronics. [(a)–(c)] Thin-film polymer electrode arrays for high-density, long-term, and multi-region recording.⁵⁸ (a) Schematic (left) and photo of the polymer-based electrode array. Left: schematic of 16-channel shank with a thickness of 14 μm . Middle: photo of a 16-channel shank (middle left) and a 4-shank, 64-channel array. Right: full view of the polymer array with 64 channels. (b) Stacks of 16 arrays for 1024-channel recording with a field programmable gate array (FPGA) headstage. (c) Left: units-per-channel statistics after implantation in rat brain show long-term recording with high yield. Right: identified units through different locations of the brain (scale bar: 200 μm and 2 ms). Reproduced with permission from Chung *et al.*, *Neuron* **101**, 21 (2019). Copyright 2019 Elsevier. [(d) and (e)] NeuroGrid for recording action potential from a rat brain surface.³¹ (d) Neurogrid on a child petal, which consists of poly(3,4-ethylenedioxythiophene):polystyrene sulfonate (PEDOT:PSS)-coated electrodes and parylene C encapsulation substrate (scale bar: 5 mm). (e) Statistics of detected action potential waveforms through more than a week post-implantation. Blue and black: recorded signal from rat hippocampus (blue) and cortex (black). Red: spike detection threshold (root mean square of noise = 8 μV at 0.1–7500 Hz). Reproduced with permission from Khodagholy *et al.*, *Nat. Neurosci.* **18**, 310 (2015). Copyright 2015 Springer Nature Limited. [(f) and (g)] A 4 \times 4 graphene solution-gated field-effect transistors (gSGFET) array (f)⁶³ and its infraslow recordings during the induction of four cortical spreading depression events [(g), blue shade]. From top to bottom: local field potential (LFP), bandpass filtered band, and voltage-converted wideband signal. Reproduced with permission from Masvidal-Codina *et al.*, *Nat. Mater.* **18**, 280 (2019). Copyright 2019 Springer Nature Limited. [(h)–(k)] Intrinsically stretchable and soft electronics based on material design. [(h) and (i)] Electronic dura mater on an intrinsically stretchable elastomeric silicone substrate.⁶⁵ (h) Photo of the device with corresponding scanning electron microscopic (SEM) characterization of the gold film and the platinum–silicone composite. (i) Recording of the signal from the cortical surface of a transgenic mouse expressing channelrhodopsin-2 (ChR2), an optogenetic protein triggered by blue light. The mouse brain is stimulated with the blue laser, and the corresponding neuron activity is recorded by electronic dura mater as shown in the cortical activation map. Reproduced with permission from Minev *et al.*, *Science* **347**, 159 (2015). Copyright 2015 The American Association for the Advancement of Science. [(j) and (k)] Intrinsically stretchable bioelectronics for neuron recording and modulation.⁷⁰ (j) Optical image of the device on rat brain's stem (the curved floor of the fourth ventricle with 50-mm electrode width) for neuromodulation. (k) Recorded muscle activity with respect to different stimulation locations of electrodes in the implanted array in the brainstem. Each muscle spike waveform is corresponding to one electrode stimulation site in the brainstem implant. Left: recorded at tongue. Middle: recorded at whisker. Right: recorded at neck. Reproduced with permission from Jiang *et al.*, *Science* **375**, 1411 (2022). Copyright 2022 The American Association for the Advancement of Science. [(l)–(q)] Tissue-like electronics.^{27,71} [(l) and (m)] Schematic illustration and confocal fluorescence imaging showing the structure similarity of neurons and mesh electronics.⁷² Reproduced with permission from Yang *et al.*, *Nat. Mater.* **18**, 510 (2019). Copyright 2019 Springer Nature Limited. [(n) and (o)] Representative 3D confocal fluorescent reconstruction of the mesh electronics within the brain after implantation showing the distribution of device (red), neuron (green), and non-neuron cells (magenta for astrocytes), indicating a seamless, gliosis-free integration of electronics with brain. [(p) and (q)] Tissue-like electronics enable tracking of the behavior-related neuron activity from the same neuron through the entire adult life of mouse. (p) Time evolution of single action potential recorded through the whole adult life of mice from month 5 to month 18. The single-unit action potential is represented with the first and second dimension of uniform manifold approximation and projection (UMAP). (q) The average waveforms of the single-unit action potential in (p). Reproduced with permission from Zhao *et al.*, *Nat. Neurosci.* (published online, 2023). Copyright 2023 Springer Nature.

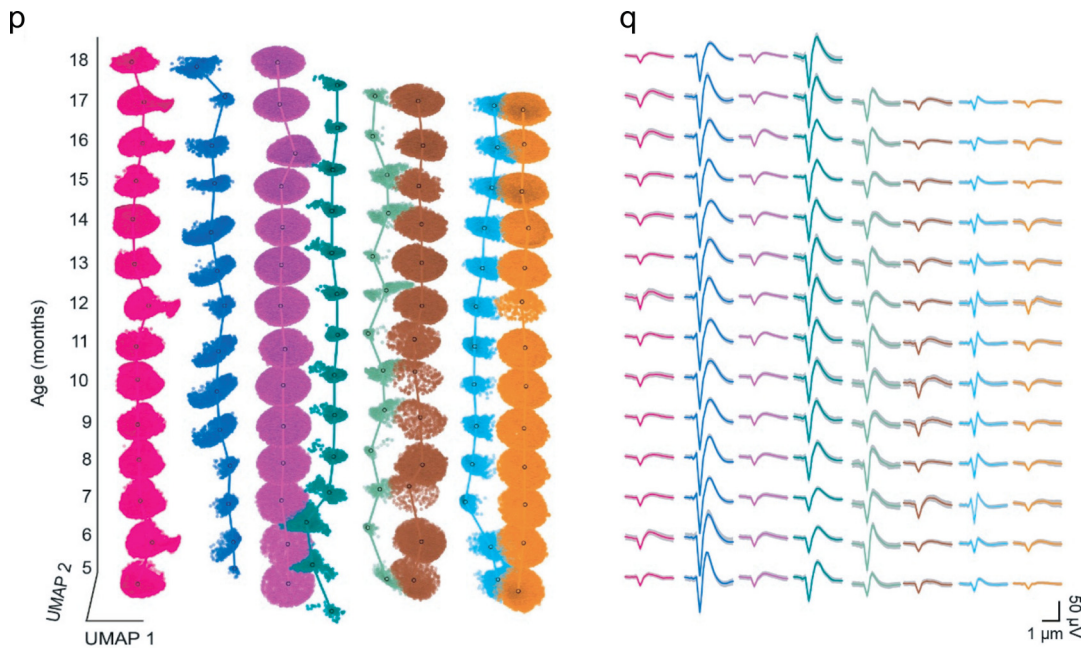


FIG. 3. (Continued.)

Using chemical modifications, Young's modulus of conductive polymers can be reduced.^{70,87,90,91} Integration of these low modulus conductive polymers into the brain probes can further reduce their rigidity.^{85,91–93} Although Young's modulus of modified soft conductive polymer materials still ranges from MPa to GPa, which is substantially larger than the brain's modulus of kPa,⁹⁴ it remains orders of magnitude smaller compared to traditional silicon-based probes, which have Young's modulus greater than 100 GPa.⁹⁵ For example, the incorporation of zonyl fluorosurfactants to the conductive polymer PEDOT:PSS will significantly reduce Young's modulus from 1.15 GPa to 338 MPa with 1% weight fraction of Zonyl.⁹⁶ Incorporation of other moieties, such as topological interlock structures, will also influence the mechanical properties of the polymeric system.^{70,97} Recently, Jiang *et al.*⁷⁰ developed an intrinsically stretchable and flexible bioelectronic device based on PEDOT:PSS with the topological-interlocked supramolecular network to form a highly conductive and stretchable electrode array [Fig. 3(j)]. The incorporation of mechanical-interlocked rotaxane into the polymer network enables larger flexibility and conformational freedom⁹⁸ together with higher conductivity due to the aggregation effect caused by PEG side chain.⁹⁹ Young's modulus of polyrotaxane-incorporated PEDOT:PSS (1:5 in dry weight, polyrotaxane:PEDOT) is reduced to ~0.8 GPa compared to pristine PEDOT:PSS as ~2.5 GPa. The authors used the PEDOT:PSS stretchable array for localized neuro-modulation of the brainstem to selectively trigger the muscle activity in the tongue, whisker, and neck [Figs. 3(j) and 3(k)].

C. Tissue-like electronics for seamless integration of electronics with tissues

In addition to the mechanical properties, the geometry and dimension of electronics also affect the bio-interface of electronics in

the brain tissue.^{73,100,101} To address this, Liu *et al.* introduced mesh-like electronics.²⁷ Unlike the standard planar structure, mesh electronics have a unique open 3D architecture where the sensors are interconnected with flexible connectors encapsulated by the sub-micrometer-thick encapsulation layers. This design mimics the structure of the tissue scaffold or neural network, which further decreases the bending stiffness of the electronics as well as allows the chemicals and biological reagents to flow freely across the implanted electronics.^{73,102–104} Zhou *et al.* systematically compared the chronic immune response of the tissues that were implanted with thin-film and mesh electronics.¹⁰² The results showed that mesh electronics could further reduce the chronic immune response to the implanted electronics. Further reduction of the feature size of the mesh electronics can be achieved by electron-beam lithography. Yang *et al.* showed that the dimension of mesh features can be reduced to the size comparable with neuron axon structures without significantly compromising the electrical performance [Figs. 3(l) and 3(m)].⁷² This design strategy offers a solution for chronically stable and gliosis-free implantation and seamless integration with biological tissues. However, the implantation of the tissue-like, tissue-level-flexible mesh electronics into the brain tissue is challenging. Initially, a syringe injection method has been developed to deliver the electronics into the brain tissue through the same process as the injection of soft biomaterials,^{33,72,105} which causes permanent damage during implantation. In addition, in the matured brain tissue, neurons innervate with each other at the nanometer scale, so the interconnected mesh network cannot fully unfold inside the brain unless in the cavity regions such as the lateral ventricle. As a result, the mesh ribbons of the electronics are bundled together, increasing the overall mechanical rigidity.^{27,33,72,102,103,105} To address this issue, Zhao *et al.* recently developed a polymer microneedle-based delivery

method, implanting and unfolding the mesh electronics across multiple regions of the mouse brain. The unfolded mesh electronics were fully integrated with the neural network after months of implantation, eliminating the immune response of the brain tissue [Figs. 3(n) and 3(o)].⁷¹ This bioelectronic interface enables chronically stable tracking of neuron activity from the same neurons throughout the adult life cycle of mice [Figs. 3(p) and 3(q)]. Based on these results, tissue-like electronics technology holds great potential for seamless integration with the brain for long-term, stable, gliosis-free recording, serving as a promising next-generation BMI.

IV. SMART ELECTRONICS FOR BMIs

A. Multimodal electronics for recording and stimulating brain activity

In addition to recording the physiological state of neurons, closed-loop BMIs require both recording and stimulation of the region of interest. Implantable electrodes can provide stimulation with moderate spatiotemporal resolution, but a more effective neurostimulation needs to target specific types of cells defined by their molecular signatures. The integration of various neurotechnologies, such as optical modulation^{106–109} and chemical modulation,^{110–114} with recording would create a valuable toolbox for multifunctional interrogation of neuron systems, with the capability for closed-loop modulation.^{38–40} For example, Yang *et al.* developed a micro LED-based wireless closed-loop BMI for optogenetic stimulation and recording in the mouse brain [Figs. 4(a) and 4(b)].¹¹⁵ Two kinds of subdermal devices include head- (HM) and back-mounted (BM) designs with microscale light-emitting diode (μ -LED) for optogenetic stimulation [Fig. 4(c)]. Aside from the optic modality, the microfluidic channel for viral delivery, pharmacology, and chemogenetics also play important roles in neuromodulation for BMIs. Park *et al.* developed a series of polymer fiber-based multifunctional bioelectronics [Fig. 4(d)] by integrating a polymer substrate, an optical waveguide, a recording electrode, and fluidic channels into single fibers.³⁸ This device realizes a functional integration of optogenetics, electrical recording, and drug delivery with chronic stability and fidelity [Figs. 4(e)–4(g)]. Similarly, a combination of fluid delivery together with optogenetic stimulation has been achieved by integrating microfluidic channels with a cellular-scale LED array [Figs. 4(h)–4(k)].³⁹ It performs multi-channel fluid delivery together with optical stimulation capability, enabling combined wireless optogenetics with pharmacology for neural circuit dissection. To illustrate the pharmacological capability, an agonist of μ -opioid receptor called [D-Ala², N-MePhe⁴, Gly-ol]-enkephalin (DAMGO) with its vehicle is injected through the multimodal electronics to ventral tegmental area (VTA) of the mouse to enable stereotypical and repeated rotation behaviors that are correlated with the increase in neuron activity [Fig. 4(m)]. Moreover, in another behavior paradigm [Figs. 4(o)–4(r)], the authors used the dopamine receptor D₁ (DRD1) antagonist SCH23390 to block the photostimulation of ChR2-induced place preference in mouse nucleus accumbens (NAc) [Fig. 4(r)], demonstrating this device as an optics-pharmacology coupling system for behavior modulation. These combined modalities provide valuable tools for closed-loop modulation of the nervous system and building up the front-end recorder/modulator part of smart electronics.

B. Wireless BMI implants

Traditional BMIs have been limited in their application due to their reliance on wired connections for data transmission. This has restricted the use of BMIs to freely behaving animals and human clinical settings. Implementation of wireless transmission to data collection could address these limitations. Simeral *et al.* have demonstrated wireless BMIs operating in human patients, fully capable of replacing the need of wires for 192 electrodes.¹¹⁶ Wireless implants eliminate the use of bulky wires and signal processing and decoding computers connected to the implant, which considerably improves the quality of life for patients in clinical applications. In addition, making the brain implants wireless enhances the stability of the connection and reduces the risk of infections or artifacts caused by external factors [Fig. 5(a)].

There are two approaches to achieving wireless data transmission for brain signals. The first approach involves directly transmitting raw data through a wireless transmission chip connected to the recording electronics. The advantage of this approach is its simplicity, as many existing electronic designs and off-the-shelf electronics can be directly integrated with the neural signal recording electronics. However, wirelessly transmitting raw neural data can be power-intensive, result in time delays, and raise privacy concerns,^{117,118} particularly given the increasing volume of data generated by high-speed, high-density, and long-term stable electrical recordings. The number of neurons simultaneously recorded with the flexible electronics has drastically increased up to thousands of channels, exponentially increasing the volume of the data needed for transmission. However, the current bandwidth for the wireless transmission of all the raw data is limited. In addition, many future BMI applications such as brain decoding, and external robotics control require real-time decoding and generation of control policy from the recorded brain signal. Therefore, smart electronics are being implemented with the brain implants, enabling on-chip decoding of neural signals and wireless transmission of processed data.

Many researchers have made efforts to enhance the intelligence of the electronics in order to conduct signal preprocessing on-chip^{119,120} [Fig. 5(b)] while consuming less power. This includes on-chip signal preprocessing, such as amplification to reduce noise, digitization via analog to digital converter (ADC), and spike detection and spike sorting. Musk and Neuralink have developed a full-packaged sensor and an application-specific integrated circuit (ASIC) that conducts several basic signal processing procedures before it is sent to an external processing station via a digital USB-C connector¹²¹ [Fig. 5(c)]. Low-power operating sensors¹²² and on-sensor data compression via compressive sensing¹²³ and compressing subsampling¹²⁴ techniques have been developed as well. Maintaining the performance of BMIs while decreasing the power consumption is the main objective for various low-power operation techniques. For this goal, identifying a few critical features from the entire neural signals that contain all the necessary information for high-performance BMI processing is a promising approach. Bansal *et al.* have identified a distinctive low-frequency LFP (δ -LFP) or the movement event-related potential, which provides sufficient information for reconstructing the kinematics of hands' grips of monkeys.¹²⁵ In addition, Mollazadeh *et al.* have shown that the spike recordings and LFP time domain amplitude give higher accuracy than frequency domain power for decoding the movement.¹²⁶ Using portion or representation of signals for transmitting and processing can reduce the power consumption and increase the performance of BMIs. For example, the high-frequency component in the range of 300–1000 Hz down sampled and smoothed

has shown similar behavioral prediction results compared to the threshold crossing rate (TCR), which allows for a significant reduction in power consumption.¹²⁷ The development of a fully implanted neural interface, which is completely isolated from the external environment,

also requires the implementation of wireless powering for the implanted device. For wireless powering of the implant, it can either receive power from an external source^{128–130} or harvest power internally.^{131,132} Jow *et al.* have built a wireless powering system inductively powered via a

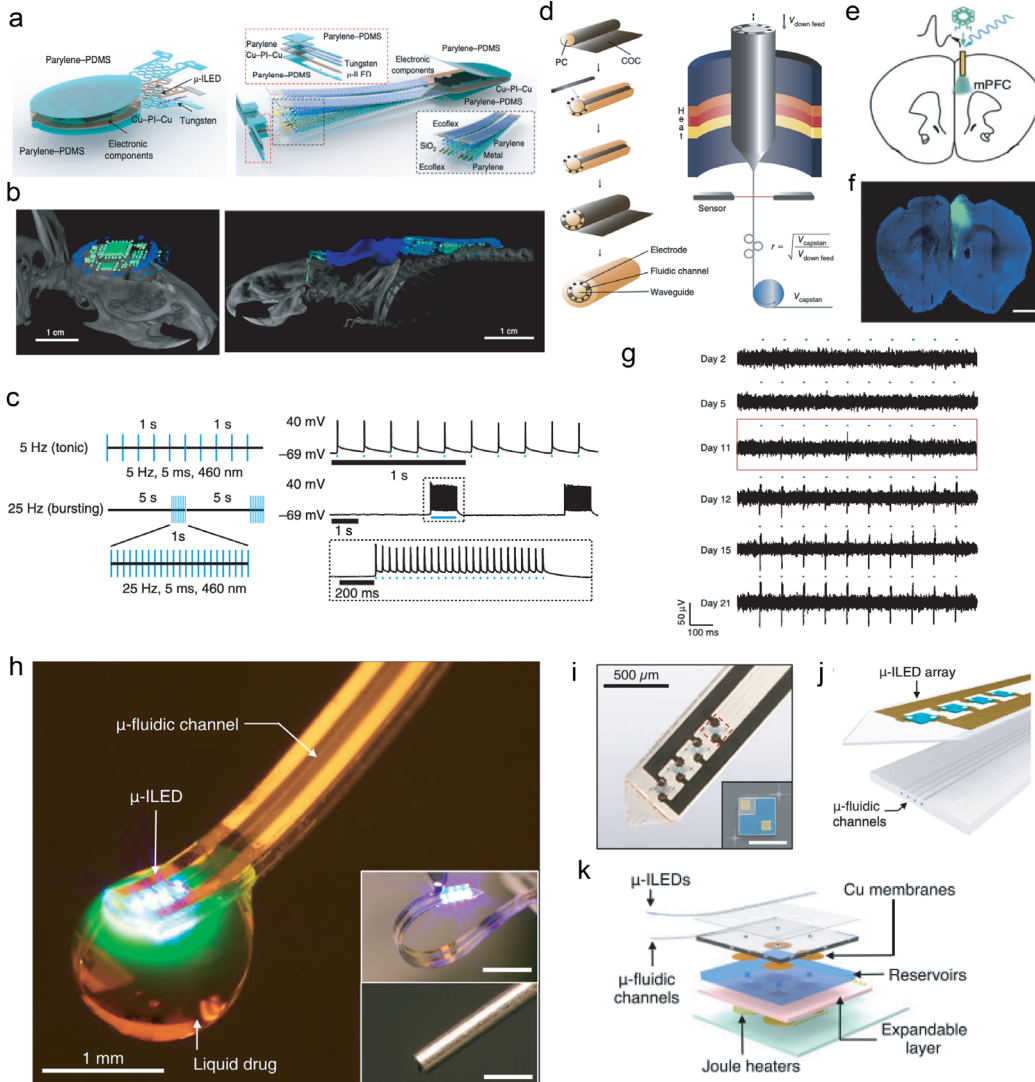


FIG. 4. Multifunctional electronics for multimodal BMIs. [(a)–(c)] Wireless LED-based electronics for the integration of optogenetic stimulation in mouse brain.¹¹⁵ (a) Schematic illustration of a wireless head-mounted (HM, left) or back-mounted (BM, right) optical stimulator. (b) Computed tomography (CT) image of HM (left) and BM (right) on a mouse brain. (c) Representative electrical recording traces with optogenetic stimulation by a current clamp recording. The wireless device is implanted into a mouse's medial prefrontal cortex (mPFC) expressing ChR2. Reproduced with permission from Yang *et al.*, *Nat. Neurosci.* **24**, 1035 (2021). Copyright 2021 Springer Nature Limited. [(d)–(g)] Multifunction fiber-based flexible BMIs for integration of optogenetic stimulation, electrical recording, and fluid delivery.³⁸ (d) Illustration of fiber assembly (left) and drawing (right) process. [(e) and (f)] Fluidic delivery of virus (AAV5-CaMKIIα-ChR2-eYFP) for the expression of ChR2 and enhanced-yellow fluorescence protein (eYFP) in excitatory neurons (e) and expression check [(f), green marks gene expression]. (g) Electrophysiological recording during optogenetic stimulation (black dots) at different times of post-implantation. Reproduced with permission from Park *et al.*, *Nat. Neurosci.* **20**, 612 (2017). Copyright 2017 Springer Nature Limited. [(h)–(q)] Wireless optofluidic system for programmable integration of optogenetics with pharmacology by integrating thin-layer neural probes with microfluidic channels and microscale inorganic light-emitting diode (μ -ILED).³⁸ (h) Photo of the μ -ILEDs array and comparison with a traditional cannula (scale bars, 1 mm). [(i) and (j)] Photo (left) and schematic illustration (right) of the optofluidic device. (k) Schematic diagram of μ -ILEDs on top of a soft microfluidic system with microfluidic channels. [(l)–(n)] Untethered delivery of [D-Ala², N-MePhe⁴, Gly-ol]-enkephalin (DAMGO) and its vehicle into VTA (ventral tegmental area) of a mouse enables stereotypical and repeated rotation behavior. [(o)–(r)] Behavior modulation. (o) Schematics showing the design of the experiment. AAV5-EF1a-DIO-ChR2-eYFP virus is injected into VTA, and SCH23390 is injected into nucleus accumbens (NAc), which is a projection downstream of VTA neurons. The optogenetic stimulation is at the axon terminal of VTA to NAc projection neurons. Dopamine receptor D₁ (DRD1) antagonist SCH23390 (SCH) will block the photostimulation of ChR2-induced place preference. [(p) and (q)] Expression of ChR2 in VTA (p) and NAc (q). (r) Place preference upon optogenetic stimulation with and without injection of SCH. Reproduced with permission from Jeong *et al.*, *Cell* **162**, 662 (2015). Copyright 2015 Elsevier.

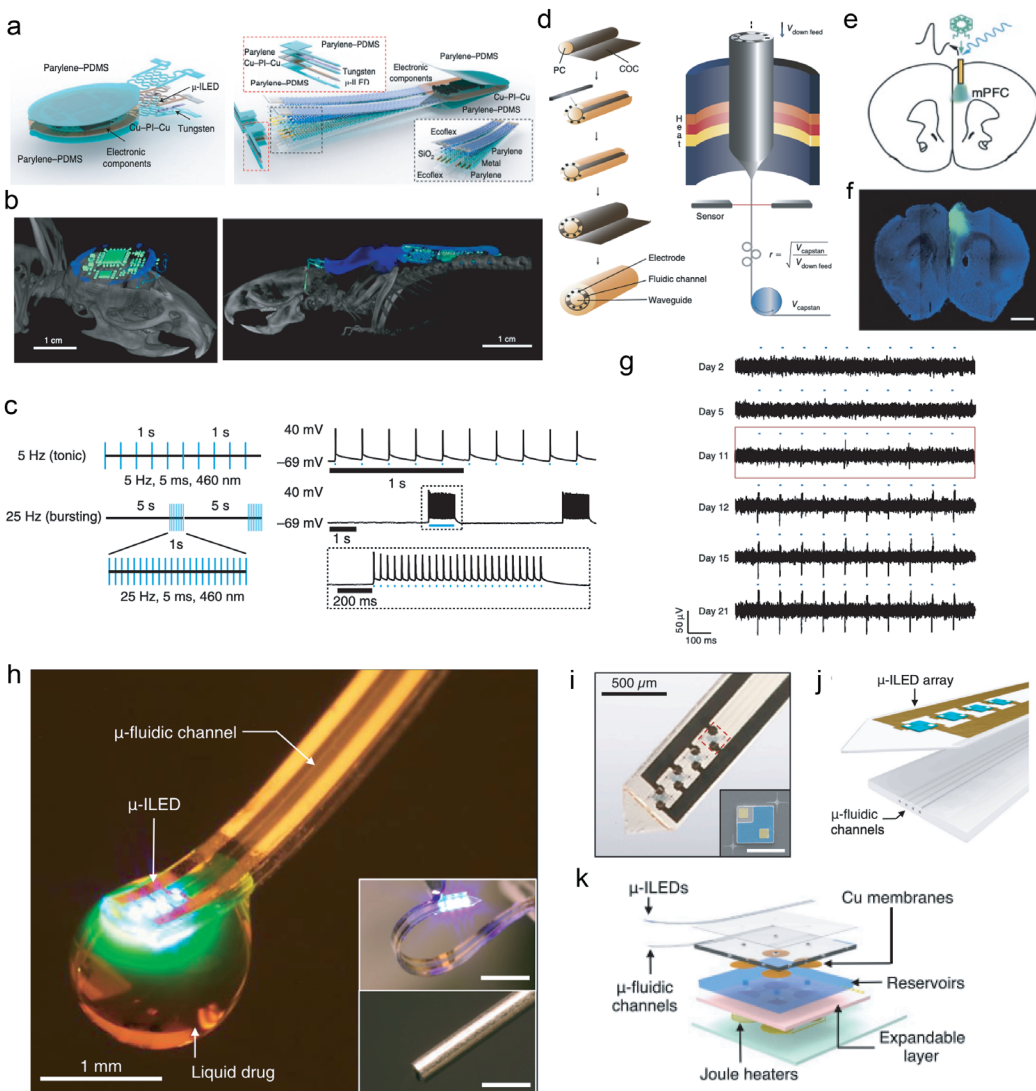


FIG. 4. (Continued.)

scalable array of overlapping planar spiral coils, achieving 20 mW continuous delivery to a freely behaving rat for more than an hour.¹³³ In addition, Ho *et al.* have developed a wireless powering method utilizing a resonant interaction between a radio frequency cavity and intrinsic modes¹³⁴ [Fig. 5(d)]. More extensive discussion on the wireless powering of BMI implants is summarized elsewhere.¹³⁵

C. BMI implants with on-chip intelligence for closed-loop operation

A promising strategy to enhance the performance of BMIs and minimize the size of the electronics required for data processing is to integrate ML algorithms into the implantable electronics. However, at the same time, it requires several strategies for effective implementation

because on-chip ML has significant limitations in various resources such as power, heat dissipation, and volume.¹¹⁷ By embedding ML capabilities within the implantable electronics, it would be possible to process neural signals on-sensor and generate control policies for stimulation, thereby enabling the development of a fully wireless, closed-loop BMI system. Further incorporating multimodal electronics that combine both sensors and multimodal stimulators would complete the structure of a completely isolated closed-loop BMI implant without the need for any external wiring^{136,137} [Fig. 5(e)].

The integration of on-chip classifiers allows for quick inference and timely input to the patients, leading to rapid and effective stimulation of the brain or control of prosthetics. Overall, the embedded ML models must process the characteristics of low-power consumption,

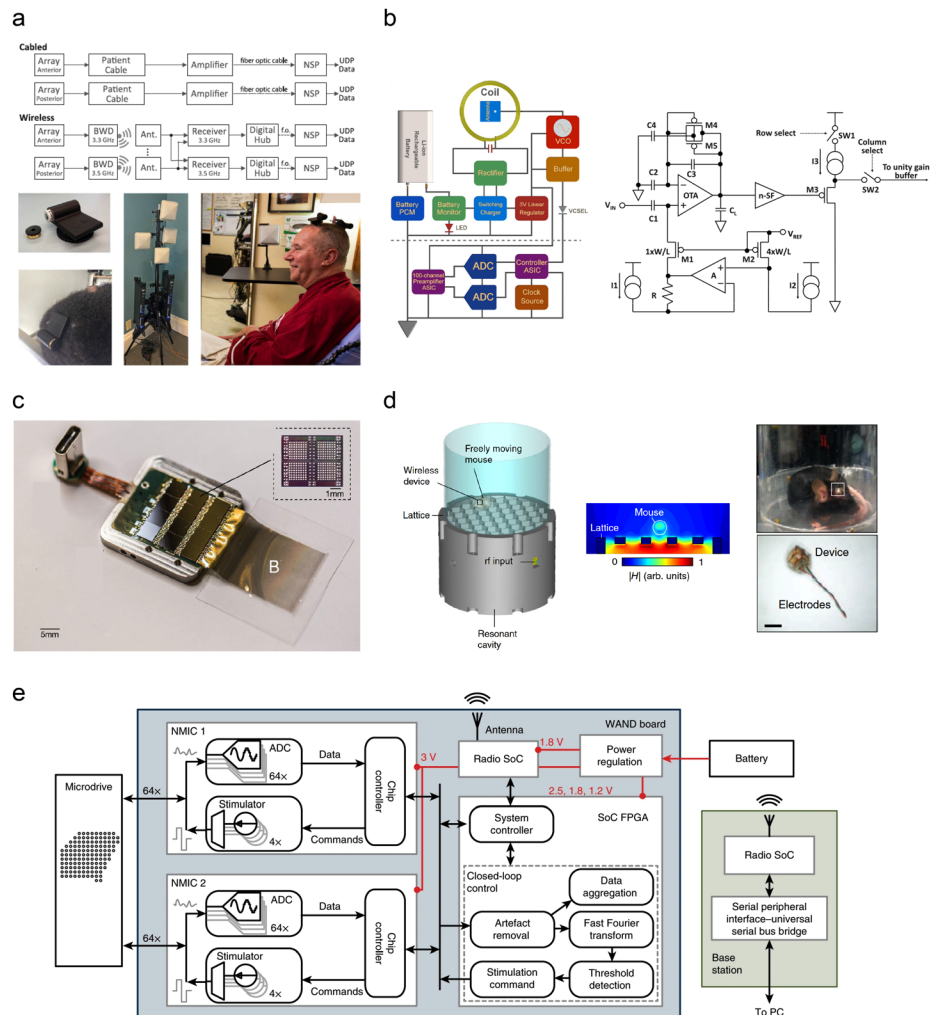


FIG. 5. Smart brain-machine interface (BMI) implants for wireless and closed-loop operation. (a) Wireless transmitters for home use of intracortical BMIs. The diagram above compares the components for cabled and wireless BMI implementing a dual-array recording. The black transmitter device shown below is called the “brown wireless device” (BWD), transmitting data with four antennas shown in the image located in the center. The participant shown in the rightmost picture is at his home with two transmitters implanted.¹¹⁶ Reproduced with permission from Simeral *et al.*, IEEE Trans. Biomed. Eng. **68**, 2313 (2021). Copyright 2021 Authors, licensed under Creative Commons Attribution-NonCommercial-NoDerivatives 4.0 International (CC BY-NC-ND 4.0) license. (b) Block diagram of both the amplification board and the transmission board of a wireless implantable module for neural signal recording (left). The circuit block diagram of the complementary metal-oxide-semiconductor (CMOS) preamplifier application-specific integrated circuit (ASIC) with 100-channels (right). The neural data are amplified, multiplexed, digitized, and packaged for transmission.¹¹⁸ Reproduced with permission from Borton *et al.*, J. Neural Eng. **10**, 026010 (2013). Copyright 2012 IOP Publishing. (c) Fully-packaged sensor and signal processing integrated circuit for high number of channels.¹²¹ Reproduced with permission from Musk *et al.*, J. Med. Internet Res. **21**, e16194 (2019). Copyright Elon Musk, Neuralink, licensed under Creative Commons Attribution License NonCommercial-NoDerivatives 4.0 International (CC BY-NC-ND 4.0) license. (d) A schematic of the self-tracking energy transfer system while the mouse freely moves (left). The distribution of magnetic field when the mouse is on top of the lattice showing the coupling between the cavity and the mouse (middle). A picture of mouse with an implanted stimulator powered wirelessly by the system (top right). The picture of the implanted device. Scale bar: 2 mm (bottom right).¹³⁴ Reproduced with permission from Ho *et al.*, Phys. Rev. Appl. **4**, 024001 (2015). Copyright 2015 American Physical Society. (e) Functional diagram of the wireless artifact-free neuromodulation device (WAND) system. The main board has neuromodulation integrated circuit (NMIC) for recording and stimulation with connections to the microdrive electrode array, battery, and wireless base station.¹³⁷ Reproduced with permission from Zhou *et al.*, Nat. Biomed. Eng. **3**, 15 (2019). Copyright 2022 Springer Nature Limited.

minimal physical footprint, and speedy detection while providing high classification accuracy. The ability to perform feature extraction and classification in real-time on the chip can enable the immediate signal processing. Cheng *et al.* have developed a 16-channel closed-loop neuromodulation system-on-chip (SoC) for controlling epileptic seizures, integrating sensors, processor, and a stimulator.¹³⁸ Their SoC is also

powered wirelessly and implements the entropy-and-spectrum algorithm with ridge regression classifier for data processing and seizure detection. The ASIC implementation of ML is particularly advantageous in BMI implants because it offers on-chip processing in real-time, giving feedback for neural stimulation, reducing data transmission rates, and reducing privacy and security issues associated

with wirelessly communicating sensitive health data. Furthermore, utilizing ML in BMIs for brain state classification or closed-loop brain stimulus treatments is showing superior performance compared to the traditional algorithms.^{42,43} It is, therefore, vital to develop a hardware-efficient ML algorithm to overcome energy and size limits on multi-channel brain implants. Yang *et al.* have developed a neural signal processor module capable of feature extractor and spike sorting for a high number of channels.¹³⁹ Designing the software and the hardware while being aware of the major hardware cost (power, area, or latency) and using model compression techniques for further optimization are also critical for BMI applications. A more extensive review on designing ML-embedded hardware for closed-loop neural implants is explained elsewhere.^{44,45}

V. OUTLOOK

The advances in flexible and smart electronics are transforming the capability of BMIs dramatically. Various strategies, such as using

intrinsically flexible and soft materials, and tissue-like electronic structures, are enabling sensing of the single-cell resolved neural signals during an extended period of time with high spatial and temporal resolution. Smart electronics with reduced power consumption can process the recording data and generate control policies *on-the-fly*, enabling fully implanted closed-loop BMIs. Despite these advances, critical challenges still exist and remain to be solved, and promising directions can be pursued.

A. Scalability of flexible sensors

Despite the human brain containing over 85×10^9 neurons, the current state of technology in BMIs only allows for the recording of a small fraction of these neurons, typically a few thousands at most. There is a pressing need to drastically increase the number of channels to even cover just a specific region of the brain for effective decoding and stimulation.¹⁴⁰ Many methods have been explored to further

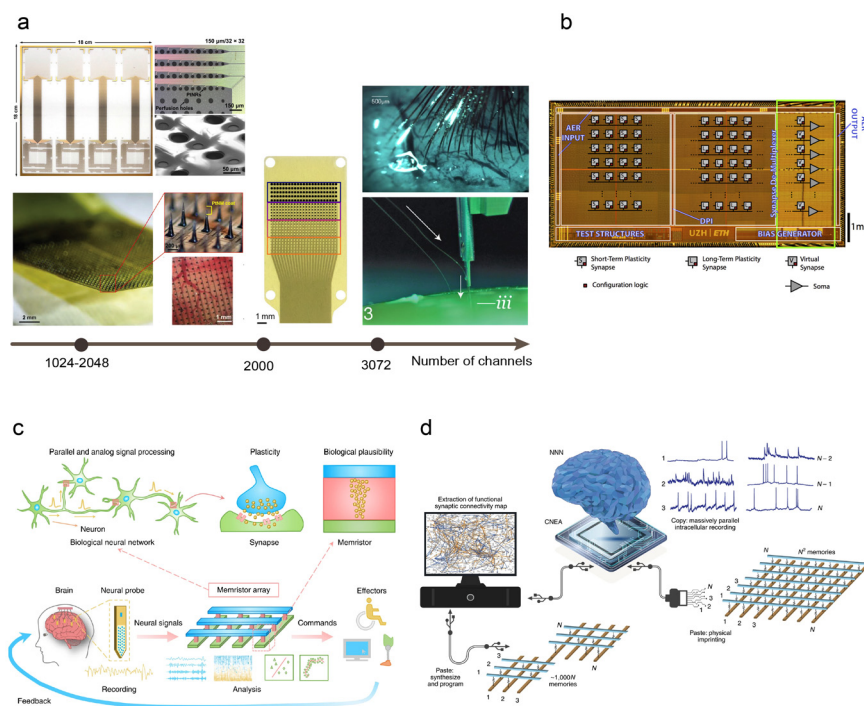


FIG. 6. Future directions for advanced brain–machine interfaces (BMIs): high-electrode-density sensors and on-chip intelligence via neuromorphic hardware. (a) Several examples of scaling up the numbers of channels in sensors recording brain activity. Studying materials and designs that can scale up in the number of channels while maintaining the flexibility is the key problem to overcome to develop long-lasting and effective BMIs. 1024-channel silicon microneedle array on flexible substrate¹⁴² [Reproduced with permission from Lee *et al.*, Adv. Funct. Mater. **32**, 2112045 (2022). Copyright 2022 Wiley-VCH GmbH.], 1024-channel platinum nanorod grid arrays¹⁴³ [Reproduced with permission from Tchoe *et al.*, Sci. Transl. Med. **14**, (2022). Copyright 2022, The American Association for the Advancement of Science.], 2000-channel microelectrode array¹⁴¹ [Reproduced with permission from Ho *et al.*, bioRxiv. Copyright 2022 Authors.], 3072 electrodes per array across 96 threads, surgical robot for automated thread insertion¹²¹ [Reproduced with permission from Musk *et al.*, J. Med. Internet Res. **21**, e16194 (2019). Copyright Elon Musk, Neuralink, licensed under Creative Commons Attribution License NonCommercial-NoDerivatives 4.0 International (CC BY-NC-ND 4.0).] (b) An example of a neuromorphic processor chip that allows for low-power processing of neural data.¹⁴⁶ Low-power processors that can support data processing of the signals measured from high number of sensors will be critical in developing wireless and smart BMIs. Reproduced with permission from Boi *et al.*, Front. Neurosci. **10**, 563 (2016). Copyright 2016 Authors, licensed under the Creative Commons Attribution License (CC BY). (c) Illustration of memristor-based analysis of brain signals.¹⁴⁵ The intrinsic similarity between biological synapses and artificial processors using memristors gives us great advantage in processing neural data. Reproduced with permission from Liu *et al.*, Nat. Commun. **11**, 4234 (2020). Copyright 2020, Authors, licensed under the Creative Commons Attribution License (CC BY). (d) Methods of storing the recorded neural signal connectivity network using various forms and types of high-density memories.¹⁴⁸ Smart BMIs could incorporate these methods of storing and utilizing the neural network recorded via the high-density, flexible BMIs. Reproduced with permission from Ham *et al.*, Nat. Electron. **4**, 635 (2021). Copyright 2021 Springer Nature Limited.

increase the number of channels^{121,141–143} [Fig. 6(a)]. This review highlights the potential benefits of using flexible and tissue-like electronics in BMIs, as they can substantially reduce the mechanical and geometrical mismatch between electronics and the brain, allowing for stable recording over an extended period of time. However, it is difficult to maintain the tissue-level flexibility of electronics while continuously scaling up the number of channels due to the intrinsic rigidity of the materials used for photolithographic fabrication. The incorporation of tissue-level soft electronic materials in brain implants could potentially solve this issue. However, all the currently available soft electronic materials are either not compatible with multilayer lithographic fabrication or not stable during long-term exposure to physiological solutions. To overcome these limitations, it is important to introduce new soft materials for brain implant fabrication and new electronic structures to further scale up the number of neurons that can be stably recorded.

When scaling up the number of recording channels, there is another issue that needs to be considered besides maintaining the overall mechanical flexibility of electronics. Increasing the number of channels will increase the invasion area during and after implantation, which can negatively affect the quality of the recorded signals. To overcome this challenge, minimizing the damage caused by the implantation process is an important direction for future BMIs. Conventional implantation techniques often require the use of stiff guiding shuttles to insert highly flexible electronics into the targeted brain region.¹⁴⁴ This becomes increasingly challenging when thousands of electrodes need to be implanted in the brain. Therefore, an automatic electrode inserter robot has been developed to address this concern.¹²¹ However, neurons in the matured brain innervate with each other at nanometer resolution. Regardless of how small and soft the brain implants are designed, mechanical damage to the fully connected neural network is inevitable. Therefore, it is important to explore new methods that could provide minimal- or even noninvasive implantation in order to preserve the integrity of the neural network.

B. Neuromorphic intelligent BMIs

When the number of recording channels is increasing, maintaining a low-power operation and wireless transmission will also be a challenge. Recently, implementation of neuromorphic devices for on-chip computing provides a promising research direction for realizing real-time, low-power on-chip processors for BMIs with high channel numbers. Neuromorphic hardware is being utilized to process neural data and build decoders [Fig. 6(b)]. Liu *et al.* used memristor arrays to conduct filtering and biomarker extraction from epilepsy-related neural signals.¹⁴⁵ The potential of neuromorphic computing is limited to the back-end analysis of brain signals. The front-end application of neuromorphic intelligent electronics for the sensing and processing of neural data near sensors is a rising research area. Boi *et al.* have created a bidirectional BMI that uses a neuromorphic processor on-chip for decoding the neural signal, exploiting the plastic synapse circuits of the neuromorphic processor to control the external device based on the recorded data.¹⁴⁶ In addition, Corradi *et al.* have developed a reconfigurable neuromorphic processor-based recording system that includes a low-noise amplifier, a delta-modulator ADC, and a band-pass filter.¹⁴⁷ Due to the intrinsic similarity between the brain and the neuromorphic hardware, it requires much less computation and, thus,

less power to record and process the neural data [Fig. 6(c)] memories.¹⁴⁸ Even further, neuromorphic hardware with high-density could lead us to efficiently storing neural network and letting us utilize the stored data to reverse-engineering our brain as a part of smart BMIs [Fig. 6(d)].

VI. CONCLUSION

In our review, we have discussed the recent developments in the field of BMIs that aim to make the devices more flexible and intelligent. The use of flexible electronics has enabled long-term, stable recording with minimized immune responses. Smart electronics, on the other hand, have enabled us to combine electrical physiology with other modalities to interrogate the brain with cell-type specificity, or to incorporate advances in electrical engineering and AI to allow for wireless and closed-loop modulation with on-chip processing. However, the current state of BMIs has limited scalability and modalities, only revealing a very small subset of the electrical and biological properties of the brain. As described previously, the brain is a highly complex system with billions of neurons with unique activity patterns spanning various timescales from millisecond to years. Therefore, to fully realize the practical applications of BMIs, it is necessary to achieve stable recording and modulation of a substantial number of neurons in a long-term, precise manner with real-time processing capabilities. Scalability, long-term stability, and the optimization of data storage, processing, and interpretation must evolve simultaneously to effectively and continuously track the substantial number of neurons through the time scale of relevant neurological processes in real-time. Moreover, leveraging other bioengineering technologies such as pharmacology, genetical engineering, and omics to achieve multimodal and cell-type specific interrogation would further enhance our understanding of the neural system and our ability to communicate with the brain.

ACKNOWLEDGMENTS

We thank J. Salant for helpful comments on the manuscript. J.L. acknowledges the support from the Harvard School of Engineering and Applied Sciences Startup Fund.

AUTHOR DECLARATIONS

Conflict of Interest

Yes, J.L. is a co-founder, scientific advisory board member, and private equity holder of Axoft.

Author Contributions

A. J. Lee and W. Wang contributed equally to this work.

Ariel J. Lee: Conceptualization (equal); Data curation (equal); Formal analysis (equal); Visualization (equal); Writing – original draft (equal); Writing – review & editing (equal). **Wenbo Wang:** Conceptualization (equal); Data curation (equal); Formal analysis (equal); Visualization (equal); Writing – original draft (equal); Writing – review & editing (equal). **Jia Liu:** Conceptualization (equal); Data curation (equal); Funding acquisition (lead); Writing – original draft (equal); Writing – review & editing (equal).

DATA AVAILABILITY

The data that support the findings of this study are available within the article.

REFERENCES

- ¹J. J. Shih, D. J. Krusinski, and J. R. Wolpaw, *Mayo Clin. Proc.* **87**, 268 (2012).
- ²J. R. Wolpaw, N. Birbaumer, D. J. McFarland, G. Pfurtscheller, and T. M. Vaughan, *Clin. Neurophysiol.* **113**, 767 (2002).
- ³J. P. Donoghue, *Neuron* **60**, 511 (2008).
- ⁴R. A. Andersen, S. Musallam, and B. Pesaran, *Curr. Opin. Neurobiol.* **14**, 720 (2004).
- ⁵F. R. Willett, D. T. Avansino, L. R. Hochberg, J. M. Henderson, and K. V. Shenoy, *Nature* **593**, 249 (2021).
- ⁶J. L. Collinger, B. Wodlinger, J. E. Downey, W. Wang, E. C. Tyler-Kabara, D. J. Weber, A. J. McMorland, M. Velliste, M. L. Boninger, and A. B. Schwartz, *Lancet* **381**, 557 (2013).
- ⁷L. R. Hochberg, D. Bacher, B. Jarosiewicz, N. Y. Masse, J. D. Simmeral, J. Vogel, S. Haddadin, J. Liu, S. S. Cash, P. van der Smagt, and J. P. Donoghue, *Nature* **485**, 372 (2012).
- ⁸G. Deuschl, C. Schade-Brittinger, P. Krack, J. Volkmann, H. Schäfer, K. Bötz, C. Daniels, A. Deutschländer, U. Dillmann, W. Eisner, D. Gruber, W. Hamel, J. Herzog, R. Hilker, S. Klebe, M. Kloß, J. Koy, M. Krause, A. Kupsch, D. Lorenz, S. Lorenzl, H. M. Mehdorn, J. R. Moringlane, W. Oertel, M. O. Pinsker, H. Reichmann, A. Reuß, G.-H. Schneider, A. Schnitzler, U. Steude, V. Sturm, L. Timmermann, V. Tronnier, T. Trottenberg, L. Wojtecki, E. Wolf, W. Poewe, and J. Voges, *N. Engl. J. Med.* **355**, 896 (2006).
- ⁹S. J. Nagel and I. M. Najm, *Neuromodulation: Technol. Neural Interface* **12**, 270 (2009).
- ¹⁰M. Vidailhet, L. Vercueil, J.-L. Houeto, P. Krystkowiak, A.-L. Benabid, P. Cornu, C. Lagrange, S. Tézenas du Montcel, D. Dormont, S. Grand, S. Blond, O. Detante, B. Pillon, C. Ardouin, Y. Agid, A. Destée, and P. Pollak, *N. Engl. J. Med.* **352**, 459 (2005).
- ¹¹S. Raspopovic, M. Capogrosso, F. M. Petrini, M. Bonizzato, J. Rigosa, G. Di Pino, J. Carpaneto, M. Controzzi, T. Boretius, E. Fernandez, G. Granata, C. M. Oddo, L. Citi, A. L. Ciancio, C. Cipriani, M. C. Carrozza, W. Jensen, E. Guglielmelli, T. Stieglitz, P. M. Rossini, and S. Micera, *Sci. Transl. Med.* **6**, 222ra19 (2014).
- ¹²D. Oude Bos and B. Reuderink, "Brainbasher: a BCI game," in *Extended Abstracts of the International Conference on Fun and Games* (Eindhoven University of Technology Eindhoven, 2008), pp. 36–39.
- ¹³A. Nijholt and D. Tan, in *Proceedings of the International Conference on Advances in Computer Entertainment Technology* (Association for Computing Machinery, New York, NY, 2007), pp. 305–306.
- ¹⁴A. Nijholt, J. B. Van Erp, and D. K. Heylen, in *Proceedings of the AISB Symposium on Brain Computer Interfaces and Human Computer Interaction: A Convergence of Ideas* (Society for the Study of Artificial Intelligence and Simulation of Behaviour, 2008), pp. 32–35.
- ¹⁵A. Nijholt, D. P.-O. Bos, and B. Reuderink, *Entertain. Comput.* **1**, 85 (2009).
- ¹⁶I. Lazarou, S. Nikolopoulos, P. C. Petrantonakis, I. Kompatsiaris, and M. Tsolaki, *Front. Hum. Neurosci.* **12**, 14 (2018).
- ¹⁷S. Machado, F. Araújo, F. Paes, B. Velasques, M. Cunha, H. Budde, L. F. Basile, R. Anghinah, O. Arias-Carrón, M. Cagy, R. Piedade, T. A. de Graaf, A. T. Sack, and P. Ribeiro, *Rev. Neurosci.* **21**, 451 (2010).
- ¹⁸G. Schalk and E. C. Leuthardt, *IEEE Rev. Biomed. Eng.* **4**, 140 (2011).
- ¹⁹K. J. Miller, D. Hermes, and N. P. Staff, *Neurosurg. Focus* **49**, E2 (2020).
- ²⁰A. Jackson and T. M. Hall, *IEEE Trans. Neural Syst. Rehabil. Eng.* **25**, 1705 (2016).
- ²¹N. A. Steinmetz, C. Aydin, A. Lebedeva, M. Okun, M. Pachitariu, M. Bauza, M. Beau, J. Bhagat, C. Böhm, M. Broux, S. Chen, J. Colonell, R. J. Gardner, B. Karsh, F. Kloosterman, D. Kostadinov, C. Mora-Lopez, J. O'Callaghan, J. Park, J. Putzeys, B. Sauerbrei, R. J. van Daal, A. Z. Volland, S. Wang, M. Welkenhuysen, Z. Ye, J. T. Dudman, B. Dutta, A. W. Hantman, K. D. Harris, A. K. Lee, E. I. Moser, J. O'Keefe, A. Renart, K. Svoboda, M. Häusser, S. Haesler, M. Carandini, and T. D. Harris, *Science* **372**, eabf4588 (2021).
- ²²Y. Ikegaya, G. Aaron, R. Cossart, D. Aronov, I. Lampl, D. Ferster, and R. Yuste, *Science* **304**, 559 (2004).
- ²³M. A. Smith and M. A. Sommer, *J. Neurosci.* **33**, 5422 (2013).
- ²⁴J. P. Seymour and D. R. Kipke, *Biomaterials* **28**, 3594 (2007).
- ²⁵R. Biran, D. C. Martin, and P. A. Tresco, *Exp. Neurol.* **195**, 115 (2005).
- ²⁶A. Gilletti and J. Muthuswamy, *J. Neural Eng.* **3**, 189 (2006).
- ²⁷J. Liu, T.-M. Fu, Z. Cheng, G. Hong, T. Zhou, L. Jin, M. Duvvuri, Z. Jiang, P. Kruskal, C. Xie, Z. Suo, Y. Fang, and C. M. Lieber, *Nat. Nanotechnol.* **10**, 629 (2015).
- ²⁸E. Song, J. Li, S. M. Won, W. Bai, and J. A. Rogers, *Nat. Mater.* **19**, 590 (2020).
- ²⁹J. Viventi, D.-H. Kim, L. Vigeland, E. S. Frechette, J. A. Blanco, Y.-S. Kim, A. E. Avrin, V. R. Tiruvadi, S.-W. Hwang, A. C. Vanleer, D. F. Wulsin, K. Davis, C. E. Gelber, L. Palmer, J. Van der Spiegel, J. Wu, J. Xiao, Y. Huang, D. Contreras, J. A. Rogers, and B. Litt, *Nat. Neurosci.* **14**, 1599 (2011).
- ³⁰D.-H. Kim, J.-H. Ahn, W. M. Choi, H.-S. Kim, T.-H. Kim, J. Song, Y. Y. Huang, Z. Liu, C. Lu, and J. A. Rogers, *Science* **320**, 507 (2008).
- ³¹D. Khodagholy, J. N. Gelinas, T. Thesen, W. Doyle, O. Devinsky, G. G. Malliaras, and G. Buzsáki, *Nat. Neurosci.* **18**, 310 (2015).
- ³²J. Liu, C. Xie, X. Dai, L. Jin, W. Zhou, and C. M. Lieber, *Proc. Natl. Acad. Sci.* **110**, 6694 (2013).
- ³³T.-M. Fu, G. Hong, T. Zhou, T. G. Schuhmann, R. D. Viveros, and C. M. Lieber, *Nat. Methods* **13**, 875 (2016).
- ³⁴H. Zeng and J. R. Sanes, *Nat. Rev. Neurosci.* **18**, 530 (2017).
- ³⁵F. Wu, E. Stark, P.-C. Ku, K. D. Wise, G. Buzsáki, and E. Yoon, *Neuron* **88**, 1136 (2015).
- ³⁶T. Kim, J. G. McCall, Y. H. Jung, X. Huang, E. R. Siuda, Y. Li, J. Song, Y. M. Song, H. A. Pao, R.-H. Kim, C. Lu, S. D. Lee, I.-S. Song, G. Shin, R. Al-Hasani, S. Kim, M. P. Tan, Y. Huang, F. G. Omenetto, J. A. Rogers, and M. R. Bruchas, *Science* **340**, 211 (2013).
- ³⁷C. Kathe, F. Michoud, P. Schönle, A. Rowald, N. Brun, J. Ravier, I. Furfarò, V. Paggi, K. Kim, S. Soloukey, L. Asboth, T. H. Hutson, I. Jelescu, A. Philippides, N. Alwahab, J. Gandar, D. Huber, C. I. De Zeeuw, Q. Barraud, Q. Huang, S. Lacour, and G. Courtine, *Nat. Biotechnol.* **40**, 198 (2022).
- ³⁸S. Park, Y. Guo, X. Jia, H. K. Choe, B. Grenja, J. Kang, J. Park, C. Lu, A. Canales, R. Chen, Y. S. Yim, G. B. Choi, Y. Fink, and P. Anikeeva, *Nat. Neurosci.* **20**, 612 (2017).
- ³⁹J.-W. Jeong, J. G. McCall, G. Shin, Y. Zhang, R. Al-Hasani, M. Kim, S. Li, J. Y. Sim, K.-I. Jang, Y. Shi, D. Y. Hong, Y. Liu, G. P. Schmitz, L. Xia, Z. He, P. Gamble, W. Z. Ray, Y. Huang, M. R. Bruchas, and J. A. Rogers, *Cell* **162**, 662 (2015).
- ⁴⁰R. Qazi, A. M. Gomez, D. C. Castro, Z. Zou, J. Y. Sim, Y. Xiong, J. Abdo, C. Y. Kim, A. Anderson, F. Lohner, S.-H. Byun, B. Chul Lee, K.-I. Jang, J. Xiao, M. R. Bruchas, and J.-W. Jeong, *Nat. Biomed. Eng.* **3**, 655 (2019).
- ⁴¹E. M. Schmidt, *Ann. Biomed. Eng.* **8**, 339 (1980).
- ⁴²D. Jaeger, S. Gilman, and J. Wayne Aldridge, *J. Neurosci. Methods* **32**, 143 (1990).
- ⁴³P. Fromherz, "Joining microelectronics and microionics: Nerve cells and brain tissue on semiconductor chips," in *ESSDERC 2007–37th European Solid State Device Research Conference* (IEEE, 2007), pp. 36–45.
- ⁴⁴Q. Qing, S. K. Pal, B. Tian, X. Duan, B. P. Timko, T. Cohen-Karni, V. N. Murthy, and C. M. Lieber, *Proc. Natl. Acad. Sci. U.S.A.* **107**, 1882 (2010).
- ⁴⁵Y. Bando, C. Grimm, V. H. Cornejo, and R. Yuste, *BMC Biol.* **17**, 71 (2019).
- ⁴⁶J. Abbott, T. Ye, K. Krenek, R. S. Gertner, S. Ban, Y. Kim, L. Qin, W. Wu, H. Park, and D. Ham, *Nat. Biomed. Eng.* **4**, 232 (2020).
- ⁴⁷B. Lefebvre, P. Yger, and O. Marre, *J. Physiol.-Paris* **110**, 327 (2016).
- ⁴⁸P. Yger, G. L. Spampinato, E. Esposito, B. Lefebvre, S. Deny, C. Gardella, M. Stimpert, F. Jetter, G. Zeck, S. Picaud, J. Duebel, and O. Marre, *ELife* **7**, e34518 (2018).
- ⁴⁹M. Zhang, Z. Tang, X. Liu, and J. Van der Spiegel, *Nat. Electron.* **3**, 191 (2020).
- ⁵⁰W. Li, D. Rodger, P. Menon, and Y.-C. Tai, *ECS Trans.* **11**, 1 (2008).
- ⁵¹M. Peuster, *Biomaterials* **24**, 4057 (2003).
- ⁵²E. Patrick, M. E. Orazem, J. C. Sanchez, and T. Nishida, *J. Neurosci. Methods* **198**, 158 (2011).
- ⁵³A. Wang, X. Liang, J. P. McAllister II, J. Li, K. Brabant, C. Black, P. Finlayson, T. Cao, H. Tang, S. O. Salley, G. W. Auner, and K. Y. Simon Ng, *J. Biomed. Mater. Res. Part A* **81A**, 363 (2007).

- ⁵⁴C. Leighton, *Nat. Mater.* **18**, 13 (2019).
- ⁵⁵B. Nketia-Yawson, H. Ahn, and J. W. Jo, *Adv. Funct. Mater.* **32**, 2108215 (2022).
- ⁵⁶C. Cea, G. D. Spyropoulos, P. Jastrzebska-Perfect, J. J. Ferrero, J. N. Gelinas, and D. Khodagholy, *Nat. Mater.* **19**, 679 (2020).
- ⁵⁷X. Xie, L. Rieth, L. Williams, S. Negi, R. Bhandari, R. Caldwell, R. Sharma, P. Tathireddy, and F. Solzbacher, *J. Neural Eng.* **11**, 026016 (2014).
- ⁵⁸J. E. Chung, H. R. Joo, J. L. Fan, D. F. Liu, A. H. Barnett, S. Chen, C. Geaghan-Breiner, M. P. Karlsson, M. Karlsson, K. Y. Lee, H. Liang, J. F. Magland, J. A. Pebbles, A. C. Tooker, L. F. Greengard, V. M. Tolosa, and L. M. Frank, *Neuron* **101**, 21 (2019).
- ⁵⁹N. Sharafkhani, A. Z. Kouzani, S. D. Adams, J. M. Long, G. Lissorgues, L. Rousseau, and J. O. Orwa, *J. Neurosci. Methods* **365**, 109388 (2022).
- ⁶⁰A. M. Lozano, N. Lipsman, H. Bergman, P. Brown, S. Chabardes, J. W. Chang, K. Matthews, C. C. McIntyre, T. E. Schlaepfer, M. Schulder, Y. Temel, J. Volkmann, and J. K. Krauss, *Nat. Rev. Neurol.* **15**, 148 (2019).
- ⁶¹M. L. Kruegelbach, N. Jenkinson, S. L. F. Owen, and T. Z. Aziz, *Nat. Rev. Neurosci.* **8**, 623 (2007).
- ⁶²R. Daneman and A. Prat, *Cold Spring Harb. Perspect. Biol.* **7**, a020412 (2015).
- ⁶³P. Carmeliet and B. De Strooper, *Nature* **485**, 451 (2012).
- ⁶⁴B. Engelhardt and R. M. Ransohoff, *Trends Immunol.* **33**, 579 (2012).
- ⁶⁵T. D. Y. Kozai, A. S. Jaquins-Gerstl, A. L. Vazquez, A. C. Michael, and X. T. Cui, *ACS Chem. Neurosci.* **6**, 48 (2015).
- ⁶⁶S. P. Lacour, G. Courtine, and J. Guck, *Nat. Rev. Mater.* **1**, 16063 (2016).
- ⁶⁷J. W. Salatino, K. A. Ludwig, T. D. Y. Kozai, and E. K. Purcell, *Nat. Biomed. Eng.* **1**, 862 (2017).
- ⁶⁸E. Masvidal-Codina, X. Illa, M. Dasilva, A. B. Calia, T. Dragojević, E. E. Vidal-Rosas, E. Prats-Alfonso, J. Martínez-Aguilar, J. M. De la Cruz, R. García-Cortadella, P. Godignon, G. Rius, A. Camassa, E. Del Corro, J. Bousquet, C. Hébert, T. Durduran, R. Villa, M. V. Sanchez-Vives, J. A. Garrido, and A. Guimerà-Brunet, *Nat. Mater.* **18**, 280 (2019).
- ⁶⁹I. R. Minev, P. Musienko, A. Hirsch, Q. Barraud, N. Wenger, E. M. Moraud, J. Gandar, M. Capogrosso, T. Milekovic, L. Asboth, R. F. Torres, N. Vachicouras, Q. Liu, N. Pavlova, S. Duis, A. Larmagnac, J. Vörös, S. Micera, Z. Suo, G. Courtine, and S. P. Lacour, *Science* **347**, 159 (2015).
- ⁷⁰Y. Jiang, Z. Zhang, Y.-X. Wang, D. Li, C.-T. Coen, E. Hwaun, G. Chen, H.-C. Wu, D. Zhong, S. Niu, W. Wang, A. Saberi, J.-C. Lai, Y. Wu, Y. Wang, A. A. Trotsuk, K. Y. Loh, C.-C. Shih, W. Xu, K. Liang, K. Zhang, Y. Bai, G. Gurusankar, W. Hu, W. Jia, Z. Cheng, R. H. Dauskardt, G. C. Gurtner, J. B.-H. Tok, K. Deisseroth, I. Soltesz, and Z. Bao, *Science* **375**, 1411 (2022).
- ⁷¹S. Zhao, X. Tang, W. Tian, *et al.*, “Tracking neural activity from the same cells during the entire adult life of mice,” *Nat. Neurosci.* (published online, 2023).
- ⁷²X. Yang, T. Zhou, T. J. Zwang, G. Hong, Y. Zhao, R. D. Viveros, T.-M. Fu, T. Gao, and C. M. Lieber, *Nat. Mater.* **18**, 510 (2019).
- ⁷³G. Hong and C. M. Lieber, *Nat. Rev. Neurosci.* **20**, 330 (2019).
- ⁷⁴X. Duan, R. Gao, P. Xie, T. Cohen-Karni, Q. Qing, H. S. Choe, B. Tian, X. Jiang, and C. M. Lieber, *Nat. Nanotechnol.* **7**, 174 (2012).
- ⁷⁵P. B. Kruskal, Z. Jiang, T. Gao, and C. M. Lieber, *Neuron* **86**, 21 (2015).
- ⁷⁶P. Berens, G. Keliris, A. Ecker, N. Logothetis, and A. Tolias, *Front. Neurosci.* **2**, 37 (2008).
- ⁷⁷M. Ganji, A. C. Paulk, J. C. Yang, N. W. Vahidi, S. H. Lee, R. Liu, L. Hossain, E. M. Arneodo, M. Thunemann, M. Shigyo, A. Tanaka, S. B. Ryu, S. W. Lee, Y. Tchoe, M. Marsala, A. Devor, D. R. Cleary, J. R. Martin, H. Oh, V. Gilja, T. Q. Gentner, S. I. Fried, E. Halgren, S. S. Cash, and S. A. Dayeh, *Nano Lett.* **19**, 6244 (2019).
- ⁷⁸L. Luan, X. Wei, Z. Zhao, J. J. Siegel, O. Potnis, C. A. Tuppen, S. Lin, S. Kazmi, R. A. Fowler, S. Holloway, A. K. Dunn, R. A. Chitwood, and C. Xie, *Sci. Adv.* **3**, e1601966 (2017).
- ⁷⁹Z. Zhao, G. D. Spyropoulos, C. Cea, J. N. Gelinas, and D. Khodagholy, *Sci. Adv.* **8**, eabm7851 (2022).
- ⁸⁰D. C. Kim, H. J. Shim, W. Lee, J. H. Koo, and D.-H. Kim, *Adv. Mater.* **32**, 1902743 (2020).
- ⁸¹J. Liu, X. Zhang, Y. Liu, M. Rodrigo, P. D. Loftus, J. Aparicio-Valenzuela, J. Zheng, T. Pong, K. J. Cyr, M. Babakhanian, J. Hasi, J. Li, Y. Jiang, C. J. Kenney, P. J. Wang, A. M. Lee, and Z. Bao, *Proc. Natl. Acad. Sci.* **117**, 14769 (2020).
- ⁸²Y. Wang, C. Zhu, R. Pfattner, H. Yan, L. Jin, S. Chen, F. Molina-Lopez, F. Lissel, J. Liu, N. I. Rabiah, Z. Chen, J. W. Chung, C. Linder, M. F. Toney, B. Murmann, and Z. Bao, *Sci. Adv.* **3**, e1602076 (2017).
- ⁸³J. Liu, J. Liu, S. Chen, T. Lei, Y. Kim, S. Niu, H. Wang, X. Wang, A. M. Foudeh, J. B.-H. Tok, and Z. Bao, *Nat. Biomed. Eng.* **3**, 58 (2019).
- ⁸⁴B. Chu, W. Burnett, J. W. Chung, and Z. Bao, *Nature* **549**, 328 (2017).
- ⁸⁵D. Khodagholy, T. Doublet, P. Quilichini, M. Gurkinkel, P. Leleux, A. Ghestem, E. Ismailova, T. Hervé, S. Sanaur, C. Bernard, and G. G. Malliaras, *Nat. Commun.* **4**, 1575 (2013).
- ⁸⁶M. Berggren and A. Richter-Dahlfors, *Adv. Mater.* **19**, 3201 (2007).
- ⁸⁷T. Someya, Z. Bao, and G. G. Malliaras, *Nature* **540**, 379 (2016).
- ⁸⁸J. Rivnay, R. M. Owens, and G. G. Malliaras, *Chem. Mater.* **26**, 679 (2014).
- ⁸⁹S. Inal, J. Rivnay, A.-O. Suiu, G. G. Malliaras, and I. McCulloch, *Acc. Chem. Res.* **51**, 1368 (2018).
- ⁹⁰R. Chen, A. Canales, and P. Anikeeva, *Nat. Rev. Mater.* **2**, 16093 (2017).
- ⁹¹J. Rivnay, S. Inal, A. Salleo, R. M. Owens, M. Berggren, and G. G. Malliaras, *Nat. Rev. Mater.* **3**, 17086 (2018).
- ⁹²J. Rivnay, P. Leleux, M. Ferro, M. Sessolo, A. Williamson, D. A. Koutsouras, D. Khodagholy, M. Ramuz, X. Strakosas, R. M. Owens, C. Benar, J.-M. Badier, C. Bernard, and G. G. Malliaras, *Sci. Adv.* **1**, e1400251 (2015).
- ⁹³Y. Kim, A. Chortos, W. Xu, Y. Liu, J. Y. Oh, D. Son, J. Kang, A. M. Foudeh, C. Zhu, Y. Lee, S. Niu, J. Liu, R. Pfattner, Z. Bao, and T.-W. Lee, *Science* **360**, 998 (2018).
- ⁹⁴S. Budday, R. Nay, R. de Rooij, P. Steinmann, T. Wyrobek, T. C. Ovaert, and E. Kuhl, *J. Mech. Behav. Biomed. Mater.* **46**, 318 (2015).
- ⁹⁵Y. Kato, S. Furukawa, K. Samejima, N. Hironaka, and M. Kashino, *Front. Neuroeng.* **5**, 11 (2012).
- ⁹⁶E. Dauzon, A. E. Mansour, M. R. Niazi, R. Munir, D.-M. Smilgies, X. Sallenave, C. Plesse, F. Goubard, and A. Amassian, *ACS Appl. Mater. Interfaces* **11**, 17570 (2019).
- ⁹⁷K. Liu, X. Zhang, D. Zhao, R. Bai, Y. Wang, X. Yang, J. Zhao, H. Zhang, W. Yu, and X. Yan, *Fundam. Res.* (in press) (2022).
- ⁹⁸Y. Okumura and K. Ito, *Adv. Mater.* **13**, 485 (2001).
- ⁹⁹D. A. Mengistie, P.-C. Wang, and C.-W. Chu, *J. Mater. Chem. A* **1**, 9907 (2013).
- ¹⁰⁰B. Tian, T. Cohen-Karni, Q. Qing, X. Duan, P. Xie, and C. M. Lieber, *Science* **329**, 830 (2010).
- ¹⁰¹Y. Park, C. K. Franz, H. Ryu, H. Luan, K. Y. Cotton, J. U. Kim, T. S. Chung, S. Zhao, A. Vazquez-Guardado, D. S. Yang, K. Li, R. Avila, J. K. Phillips, M. J. Quezada, H. Jang, S. S. Kwak, S. M. Won, K. Kwon, H. Jeong, A. J. Bandodkar, M. Han, H. Zhao, G. R. Osher, H. Wang, K. Lee, Y. Zhang, Y. Huang, J. D. Finan, and J. A. Rogers, *Sci. Adv.* **7**, eabf9153 (2021).
- ¹⁰²T. Zhou, G. Hong, T.-M. Fu, X. Yang, T. G. Schuhmann, R. D. Viveros, and C. M. Lieber, *Proc. Natl. Acad. Sci.* **114**, 5894 (2017).
- ¹⁰³G. Hong, X. Yang, T. Zhou, and C. M. Lieber, *Curr. Opin. Neurobiol.* **50**, 33 (2018).
- ¹⁰⁴J. Rivnay, H. Wang, L. Fenno, K. Deisseroth, and G. G. Malliaras, *Sci. Adv.* **3**, e1601649 (2017).
- ¹⁰⁵G. Hong, T.-M. Fu, M. Qiao, R. D. Viveros, X. Yang, T. Zhou, J. M. Lee, H.-G. Park, J. R. Sanes, and C. M. Lieber, *Science* **360**, 1447 (2018).
- ¹⁰⁶E. S. Boyden, F. Zhang, E. Bamberg, G. Nagel, and K. Deisseroth, *Nat. Neurosci.* **8**, 1263 (2005).
- ¹⁰⁷K. Deisseroth, *Nat. Methods* **8**, 26 (2011).
- ¹⁰⁸V. Emiliani, E. Entcheva, R. Hedrich, P. Hegemann, K. R. Konrad, C. Lüscher, M. Mahn, Z.-H. Pan, R. R. Sims, J. Vierock, and O. Yizhar, *Nat. Rev. Methods Primers* **2**, 55 (2022).
- ¹⁰⁹M. Häusser, *Nat. Methods* **11**, 1012 (2014).
- ¹¹⁰G. Forkmann and B. Dangelmayr, *Biochem. Genet.* **18**, 519 (1980).
- ¹¹¹G. M. Alexander, S. C. Rogan, A. I. Abbas, B. N. Armbruster, Y. Pei, J. A. Allen, R. J. Nonneman, J. Hartmann, S. S. Moy, M. A. Nicolelis, J. O. McNamara, and B. L. Roth, *Neuron* **63**, 27 (2009).
- ¹¹²J. L. Gomez, J. Bonaventura, W. Lesniak, W. B. Mathews, P. Sysa-Shah, L. A. Rodriguez, R. J. Ellis, C. T. Richie, B. K. Harvey, R. F. Dannals, M. G. Pomper, A. Bonci, and M. Michaelides, *Science* **357**, 503 (2017).
- ¹¹³B. L. Roth, *Neuron* **89**, 683 (2016).
- ¹¹⁴S. M. Sternson and B. L. Roth, *Annu. Rev. Neurosci.* **37**, 387 (2014).
- ¹¹⁵Y. Yang, M. Wu, A. Vázquez-Guardado, A. J. Wegener, J. G. Grajales-Reyes, Y. Deng, T. Wang, R. Avila, J. A. Moreno, S. Minkowicz, V. Dumrongprachachan,

- J. Lee, S. Zhang, A. A. Legaria, Y. Ma, S. Mehta, D. Franklin, L. Hartman, W. Bai, M. Han, H. Zhao, W. Lu, Y. Yu, X. Sheng, A. Banks, X. Yu, Z. R. Donaldson, R. W. Gereau, C. H. Good, Z. Xie, Y. Huang, Y. Kozorovitskiy, and J. A. Rogers, *Nat. Neurosci.* **24**, 1035 (2021).
- ¹¹⁶J. D. Simeral, T. Hosman, J. Saab, S. N. Flesher, M. Vilela, B. Franco, J. N. Kelemen, D. M. Brandman, J. G. Ciancibello, P. G. Rezaii, E. N. Eskandar, D. M. Rosler, K. V. Shenoy, J. M. Henderson, A. V. Nurmikko, and L. R. Hochberg, *IEEE Trans. Biomed. Eng.* **68**, 2313 (2021).
- ¹¹⁷J. Yoo and M. Shoaran, *Curr. Opin. Biotechnol.* **72**, 95 (2021).
- ¹¹⁸S. Burwell, M. Sample, and E. Racine, *BMC Med. Ethics* **18**, 60 (2017).
- ¹¹⁹D. A. Borton, M. Yin, J. Aceros, and A. Nurmikko, *J. Neural Eng.* **10**, 026010 (2013).
- ¹²⁰C. A. Chestek, V. Gilja, P. Nuyujukian, R. J. Kier, F. Solzbacher, S. I. Ryu, R. R. Harrison, and K. V. Shenoy, *IEEE Trans. Neural Syst. Rehabil. Eng.* **17**, 330 (2009).
- ¹²¹E. Musk and Neuralink, *J. Med. Internet Res.* **21**, e16194 (2019).
- ¹²²N. Even-Chen, D. G. Muratore, S. D. Stavisky, L. R. Hochberg, J. M. Henderson, B. Murmann, and K. V. Shenoy, *Nat. Biomed. Eng.* **4**, 984 (2020).
- ¹²³M. Shoaran, M. M. Lopez, V. S. R. Pasupureddi, Y. Leblebici, and A. Schmid, in *Proceedings of the IEEE International Symposium on Circuits and Systems (ISCAS)* (IEEE, 2013), pp. 2191–2194.
- ¹²⁴C. Aprile, K. Ture, L. Baldassarre, M. Shoaran, G. Yilmaz, F. Maloberti, C. Dehollain, Y. Leblebici, and V. Cevher, *IEEE Trans. Circuits Syst. I Regul. Pap.* **65**, 3929 (2018).
- ¹²⁵A. K. Bansal, C. E. Vargas-Irwin, W. Truccolo, and J. P. Donoghue, *J. Neurophysiol.* **105**, 1603 (2011).
- ¹²⁶M. Mollazadeh, V. Aggarwal, A. G. Davidson, A. J. Law, N. V. Thakor, and M. H. Schieber, *J. Neurosci.* **31**, 15531 (2011).
- ¹²⁷S. R. Nason, A. K. Vaskov, M. S. Willsey, E. J. Welle, H. An, P. P. Vu, A. J. Bullard, C. S. Nu, J. C. Kao, K. V. Shenoy, T. Jang, H.-S. Kim, D. Blaauw, P. G. Patil, and C. A. Chestek, *Nat. Biomed. Eng.* **4**, 973 (2020).
- ¹²⁸J. Ausra, M. Wu, X. Zhang, A. Vázquez-Guardado, P. Skelton, R. Peralta, R. Avila, T. Murickan, C. R. Haney, Y. Huang, J. A. Rogers, Y. Kozorovitskiy, and P. Gutruf, *Proc. Natl. Acad. Sci.* **118**, e2025775118 (2021).
- ¹²⁹C. T. Wentz, J. G. Bernstein, P. Monahan, A. Guerra, A. Rodriguez, and E. S. Boyden, *J. Neural Eng.* **8**, 046021 (2011).
- ¹³⁰Y. Rajavi, M. Taghivand, K. Aggarwal, A. Ma, and A. S. Y. Poon, *IEEE J. Solid-State Circuits* **52**, 1221 (2017).
- ¹³¹K. T. Settaluri, H. Lo, and R. J. Ram, *J. Electron. Mater.* **41**, 984 (2012).
- ¹³²G.-T. Hwang, Y. Kim, J.-H. Lee, S. Oh, C. Kyu Jeong, D. Y. Park, J. Ryu, H. Kwon, S.-G. Lee, B. Joung, D. Kim, and K. Jae Lee, *Energy Environ. Sci.* **8**, 2677 (2015).
- ¹³³U.-M. Jow, P. McMenamin, M. Kiani, J. R. Manns, and M. Ghovanloo, *IEEE Trans. Biomed. Eng.* **61**, 139 (2014).
- ¹³⁴J. S. Ho, Y. Tanabe, S. M. Iyer, A. J. Christensen, L. Grosenick, K. Deisseroth, S. L. Delp, and A. S. Y. Poon, *Phys. Rev. Appl.* **4**, 024001 (2015).
- ¹³⁵S. M. Won, L. Cai, P. Gutruf, and J. A. Rogers, *Nat. Biomed. Eng.* **1**, 1–19 (2021).
- ¹³⁶X. Liu, M. Zhang, A. G. Richardson, T. H. Lucas, and J. Van der Spiegel, *IEEE Trans. Biomed. Circuits Syst.* **11**, 729 (2017).
- ¹³⁷A. Zhou, S. R. Santacruz, B. C. Johnson, G. Alexandrov, A. Moin, F. L. Burghardt, J. M. Rabaey, J. M. Carmena, and R. Muller, *Nat. Biomed. Eng.* **3**, 15 (2019).
- ¹³⁸C.-H. Cheng, P.-Y. Tsai, T.-Y. Yang, W.-H. Cheng, T.-Y. Yen, Z. Luo, X.-H. Qian, Z.-X. Chen, T.-H. Lin, W.-H. Chen, W.-M. Chen, S.-F. Liang, F.-Z. Shaw, C.-S. Chang, Y.-L. Hsin, C.-Y. Lee, M.-D. Ker, and C.-Y. Wu, *IEEE J. Solid-State Circuits* **53**, 3314 (2018).
- ¹³⁹Y. Yang, S. Boling, and A. J. Mason, *IEEE Trans. Biomed. Circuits Syst.* **11**, 743 (2017).
- ¹⁴⁰P. Le Floch, N. Molinari, K. Nan, S. Zhang, B. Kozinsky, Z. Suo, and J. Liu, *Nano Lett.* **20**, 224 (2020).
- ¹⁴¹E. Ho, M. Hettick, D. Papageorgiou, A. J. Poole, M. Monge, M. Vomero, K. R. Gelman, T. Hanson, V. Tolosa, M. Mager, and B. I. Rapoport, *bioRxiv*.
- ¹⁴²S. H. Lee, M. Thunemann, K. Lee, D. R. Cleary, K. J. Tonsfeldt, H. Oh, F. Azzazy, Y. Tchoe, A. M. Bourhis, L. Hossain, Y. G. Ro, A. Tanaka, K. Kılıç, A. Devor, and S. A. Dayeh, *Adv. Funct. Mater.* **32**, 2112045 (2022).
- ¹⁴³Y. Tchoe, A. M. Bourhis, D. R. Cleary, B. Stedelin, J. Lee, K. J. Tonsfeldt, E. C. Brown, D. A. Siler, A. C. Paulk, J. C. Yang, H. Oh, Y. G. Ro, K. Lee, S. M. Russman, M. Ganji, I. Galton, S. Ben-Haim, A. M. Raslan, and S. A. Dayeh, *Sci. Transl. Med.* **14**, eabj1441 (2022).
- ¹⁴⁴X. Wei, L. Luan, Z. Zhao, X. Li, H. Zhu, O. Potnis, and C. Xie, *Adv. Sci.* **5**, 1700625 (2018).
- ¹⁴⁵Z. Liu, J. Tang, B. Gao, P. Yao, X. Li, D. Liu, Y. Zhou, H. Qian, B. Hong, and H. Wu, *Nat. Commun.* **11**, 4234 (2020).
- ¹⁴⁶F. Boi, T. Moraitis, V. De Feo, F. Diotalevi, C. Bartolozzi, G. Indiveri, and A. Vato, *Front. Neurosci.* **10**, 563 (2016).
- ¹⁴⁷F. Corradi, D. Bontrager, and G. Indiveri, in *Proceedings of the IEEE Biomedical Circuits and Systems (BioCAS)* (IEEE, 2014), pp. 584–587.
- ¹⁴⁸D. Ham, H. Park, S. Hwang, and K. Kim, *Nat. Electron.* **4**, 635 (2021).